

Supplementary Information

Target-Oriented Design and Biosynthesis of Thiostrepton-Derived Thiopeptide Antibiotics with Improved Pharmaceutical Properties

Shoufeng Wang^{1#}, Qingfei Zheng^{1#}, Jianfeng Wang², Zhixiong Zhao¹, Qingye Li³, Yunsong Yu²,
Renxiao Wang¹, and Wen Liu^{1,3*}

¹ State Key Laboratory of Bioorganic and Natural Products Chemistry, Shanghai Institute of Organic Chemistry, Chinese Academy of Sciences, 345 Lingling Road, Shanghai 200032, China

² Department of Infectious Diseases, Sir Run Run Shaw Hospital, College of Medicine, Zhejiang University, Hangzhou, Zhejiang 310016, China

³ Huzhou Center of Bio-Synthetic Innovation, 1366 Hongfeng Road, Huzhou 313000, China

[#] These Authors equally contributed to this work.

* To whom correspondence should be addressed: Shanghai Institute of Organic Chemistry, Chinese Academy of Sciences, 345 Lingling Rd., Shanghai 200032, China. Wen Liu, Email: wliu@mail.sioc.ac.cn, Tel: 86-21-54925111, Fax: 86-21-64166128

Table of Contents

1. Supplementary Methods

- 1.1. General materials and methods**
- 1.2. Theoretical calculations and molecular modeling**
- 1.3. Precursor synthesis for chemical feeding**
- 1.4. Fermentation, chemical feeding, compound analysis and isolation**
- 1.5. In vitro anti-infective assays**
- 1.6. Determination of compound water solubility**

2. Supplementary Results

- 2.1. Characterization of synthetic precursors for chemical feeding**
- 2.2. Characterization of TSR derivatives**
- 2.3. Supplementary Tables**
 - Table S1. Bacteria strains used in this study**
 - Table S2. ^1H and ^{13}C NMR assignments of 5'-fluoro-TSR**
 - Table S3. ^1H and ^{13}C NMR assignments of 12'-methyl-TSR**
 - Table S4. The in silico screen and molecular modeling of the interaction between modified QA moiety and A1067**
- 2.4. Supplementary Figures**
 - Fig. S1. Isocontour plot in mesh of $\Delta\rho_{\text{QA-A}} = \rho_{\text{QA-A}} - \rho_{\text{QA}} - \rho_{\text{A}}$ for TSR**
 - Fig. S2. Two-layer model for optimization in Gaussian**
 - Fig. S3. Proposed biosynthetic pathway for QA formation and incorporation**
 - Fig. S4. Ultraviolet absorption of 5'-fluoro-TSR (a) and 12'-methyl-TSR (b)**
 - Fig. S5. 1D and 2D NMR spectra of 5'-fluoro-TSR**
 - Fig. S6. 1D and 2D NMR spectra of 12'-methyl-TSR**
 - Fig. S7. NMR analysis of methyl quinoline-2-carboxylates and its analogues**
 - Fig. S8. NMR analysis of methyl 4-acetyl-quinoline-2-carboxylate and its analogues**

3. Supplementary References

1. Supplementary Methods

1.1. General materials and methods

Biochemicals and media were purchased from Sinopharm Chemical Reagent Co., Ltd. (Shanghai, China) unless otherwise noted. All commercially available reagents and solvents were used without further purification unless otherwise noted. Analytical thin layer chromatography (TLC) was performed on DC-Alufolien Kieselgel 60F₂₅₄ 0.2 mm plates (Merck), and compounds were visualized by UV fluorescence. ¹H NMR, ¹³C NMR and ¹⁹F NMR spectra were recorded on a Bruker AC-400 or Bruker AC-500 spectrometer using deuterated solvents and were referenced internally to the residual solvent peak signal. Coupling constants (*J*-values) are given in hertz (Hz). NMR spectra peak assignment was aided by comparison with the literature values for similar compounds. High-performance liquid chromatography (HPLC) analysis was performed on an Agilent™ 1200 HPLC system (Agilent Technologies Inc., USA). The measurement of UV-visible absorbance was conducted using a JASCO V-530 spectrophotometer (Tokyo, Japan). Electrospray ionization MS (ESI-MS) was performed on a Thermo Fisher LTQ Fleet ESI-MS spectrometer (Thermo Fisher Scientific Inc., USA). High-resolution MS (HRMS) analysis was conducted on an IonSpec 4.7 Tesla FTMS (IonSpec, Lake Forest, CA). Taq DNA Polymerase (P101-d3) and pUM19-T Simple Vector (C403-03) used to determine the genotypes were purchased from Vazyme Biotech Co., Ltd. (Nanjing, China).

1.2. Theoretical calculations and molecular modeling

1.2.1 Analysis of electron density properties

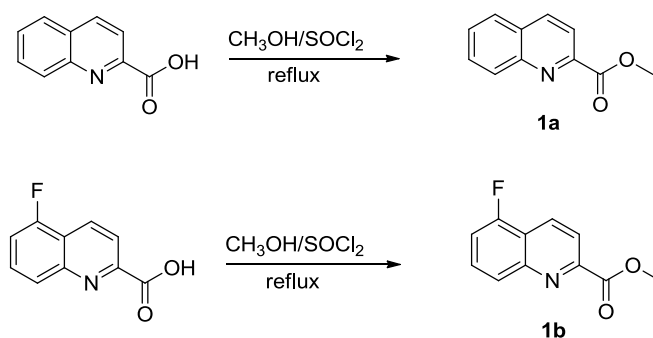
Analysis of electron density properties was performed by Gaussian 09 at M062X/6-311++g(d,p) level for the QA and adenine (A1067) residues. The difference of electron density between the two residue in complex and individual residues ($\Delta\rho_{QA-A} = \rho_{QA-A} - \rho_{QA} - \rho_A$) was calculated by the cubegen and cubman programs in Gaussian (**Fig. S1**).

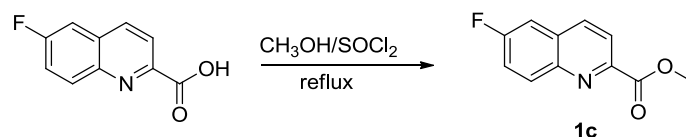
1.2.2. Quantum Mechanics (QM)-Molecular Mechanics (MM) modeling

The crystal structure of TSR in complex with L11 and 23S RNA (PDB code: 3CF5)¹ was used as the template to derive the binding modes of 6'-fluoro-TSR, 5'-fluoro-TSR, and 12'-methyl-TSR to L11 and 23S RNA. The QA moiety of TSR was modified as appropriate to yield those of 6'-fluoro-TSR, 5'-fluoro-TSR, and 12'-methyl-TSR. The resulting structures of 6'-fluoro-TSR, 5'-fluoro-TSR, and 12'-methyl-TSR were then optimized with the MMFF94x force field in the MOE software (version 2012, released by CCG) To obtain more accurate complex structures, the two-layered ONIOM method^{2,3} (M062X⁴:HF) implemented in the Gaussian 09 software⁵ was used to further optimize the modified QA moieties of 6'-fluoro-TSR, 5'-fluoro-TSR, and 12'-methyl-TSR within the constraints of the TSR binding pocket (**Fig. S2**). The QA moiety of TSR, the adenine residue interacting with it and two more linking atoms were set as the high-level layer. The residues within 5 Å from the high-level layer were set as the low-level layer, which were kept fixed during structural optimization. The high-level layer was processed at the M062X/6-31+G(d,p) level, while the low-level layer was processed at the HF/3-21G level in ONIOM calculation.

1.3. Precursor synthesis for chemical feeding

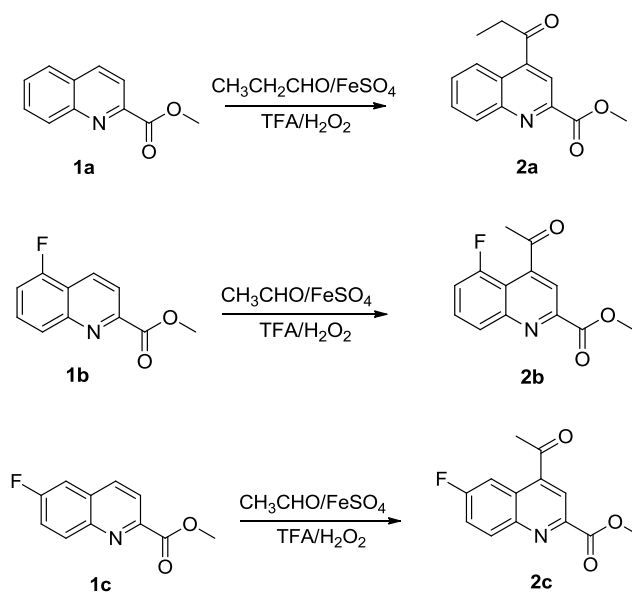
1.3.1 Synthesis of methyl quinoline-2-carboxylate and its analogues





The synthesis was carried out according to a method described previously⁶. Quinoline-2-carboxylic acid (10.0 mmol) was dissolved in dry MeOH and placed in an ice bath. SOCl₂ (0.92 mL, 12.0 mmol) was then added dropwise, and the corresponding mixture was refluxed overnight until the starting material was undetectable upon TLC analysis. The suspension was cooled to room temperature and then carefully poured into aqueous saturated NaHCO₃ solution. The resulting mixture was extracted twice with CH₂Cl₂. The organic extracts were combined, dried over anhydrous Na₂SO₄, and filtered, and the solvent was then removed by evaporation under vacuum. The resulting residue was purified by column chromatography to obtain the pure ester.

1.3.2 Synthesis of methyl 4-acetyl-quinoline-2-carboxylate and its analogues



The synthesis was carried out according to a method described previously⁶. FeSO₄•7H₂O (0.38 g, 1.37 mmol) was added to a solution of methyl quinoline-2-carboxylate (10 mmol) in TFA (0.97 mL) and acetaldehyde (50 mL), and the resulting mixture was cooled to 0 °C. An initial portion of a 30% aqueous solution of H₂O₂ (5.5 mL) was slowly added dropwise, and the mixture was stirred

for 30 min. A second portion of 30% aqueous H₂O₂ (5.5 mL) was then slowly added dropwise, and the resulting mixture was stirred for an additional 90 min. After warming to 25 °C, the reaction mixture was slowly quenched with 5% aqueous Na₂S₂O₃ solution (50 mL) followed by the addition of saturated aqueous NaHCO₃ solution. The aqueous layer was extracted with EtOAc, and the combined organic layers were washed with brine, dried over anhydrous Na₂SO₄, and filtered. The solvent was then removed by evaporation under vacuum. The resulting residue was purified by column chromatography to obtain the pure product.

1.4. Fermentation, chemical feeding, compound analysis and isolation

1.4.1 Fermentation

The fermentation was conducted according to a method described previously⁷. The $\Delta TsrT$ mutant *Streptomyces laurentii* strain SL1102 was grown in a flask containing seed medium [15 g/L Soluble starch, 15 g/L tryptic soy broth, 50 g/L sucrose, pH 7.2] (50 mL) for 2 days at 28 °C and 220 rpm. The seed culture (5 mL each) was used to inoculate ten flasks (500 mL) containing fermentation medium [15 g/L tryptic soy broth, 15 g/L CaSO₄, 11 g/L yeast extra, 50 g/L glucose, pH 7.2] (100 mL). To produce TSR and its derivatives, the medium was supplemented with methyl 4-acetyl-quinoline-2-carboxylate and its analogs (2 mg dissolved in 2 mL MeOH) and incubated at 28 °C and 220 rpm for 3 days.

1.4.2 Compound analysis

After 3 days of incubation, the cultures were centrifuged and the mycelium cake was soaked with acetone overnight. The acetone was evaporated using a rotary evaporator, and the product was dissolved in chloroform. Samples were analyzed by HPLC with a ZORBAX SB-C18 column (250 x 4.6 mm, 5 µm). The column was eluted with solvents A (water) and B (acetonitrile) at a flow rate of 1 mL min⁻¹ as follows: 0 to 3 min, constant 85% A/15% B; 3 to 6 min, a linear gradient from 85% A/15% B to 60% A/40% B; 6 to 12 min, constant 60% A/40% B; 12 to 19 min, a linear gradient from 60% A/40% B to 45% A/55% B; 19 to 22 min, a linear gradient from 45% A/55% B

to 15% A/86% B; 22 to 28 min, constant 15% A/86% B; and 28 to 35 min, a linear gradient from 15% A/86% B to 85% A/15% B. Absorbance was monitored at 254 nm.

1.4.3 Compound isolation

To obtain purified 5'-fluoro-TSR or 12'-methyl-TSR, the crude extracts were subjected to silica gel chromatography eluting with 100% CHCl₃ followed by CHCl₃-MeOH (100:1 to 100:10). Fractions containing the TSR derivative were pooled, and the organic solvent was evaporated to give the pure products. Purified samples were analyzed by HPLC-MS, HRMS, and NMR and then stored at -20 °C.

1.5. In vitro anti-infective assays

The minimum inhibitory concentrations (MIC) of TSR and its derivatives were determined by the broth microdilution method⁸ by using the normal inoculum of 0.5 MacFarland diluted 1:100 to make a final concentration of 5×10^5 CFU/mL (calculated according to the 0.5 McFarland standard (McFarland, 1907)). Each tested compound was dissolved in DMSO to produce a stock solution (100 µg/mL), which was serially diluted into 100 µL of Mueller-Hinton broth (Qingdao Hope Bio-Technology Co. Ltd., China) in a 96-well micro-titer plate to final concentrations ranging from 1 to 0 µg/mL. A 100 µL aliquot of the test strain was then added to each well of the microtiter plate. After incubation at 37 °C for 18 to 24 h, the MIC was considered the lowest concentration of compound that inhibited visible bacterial growth. The MIC of colistin was measured with an E-test (AB bioMérieux, Solna, Sweden). The manipulations and interpretations were in accordance with the descriptions of the Clinical and Laboratory Standard Institute (CLSI 2011)⁹.

1.6. Determination of water solubility

The solubility was measured according to a 'saturation shake-flask method' described previously⁸. To determine the solubility of TSR, 5'-fluoro-TSR, 6'-fluoro-TSR, and 12'-methyl-TSR, 3 mg of

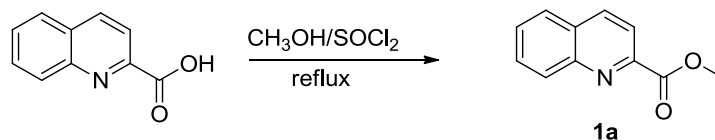
solid was added to 1 mL of water in a vial. The vial was gently stirred over a 24-h period at 30 °C to ensure the solution was at equilibrium. A 0.22- μm centrifugal filter unit (Millipore Ultrafree-MC, USA) was used for filtration to remove the excess solid. The saturated solution was then subjected to HPLC analysis to determine the concentration of the sample based on the established calibration curve. To establish the calibration curve, a set of solutions of varying concentrations of TSR, 5'-fluoro-TSR, 6'-fluoro-TSR, and 12'-methyl-TSR were analyzed independently by HPLC. The peak areas as a function of concentration were fitted to a regression equation, resulting in a linear standard curve for estimating the concentrations of the unknowns. The solubility of each compound was measured 5 times.

2. Supplementary Results

2.1. Characterization of synthetic precursors for chemical feeding

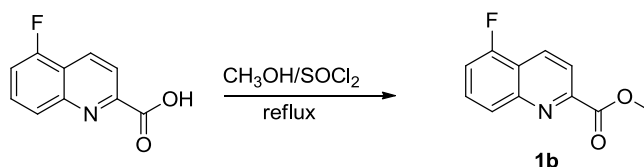
2.1.1. Characterization of methyl quinoline-2-carboxylate and its analogues

Methyl quinoline-2-carboxylate (1a)



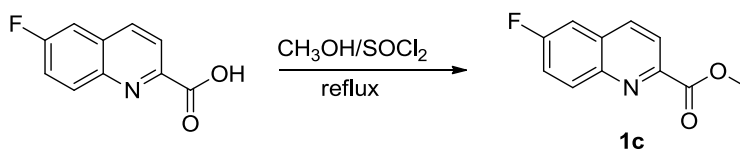
1a (1.59 g, 85.1%). ¹H NMR(500 MHz, CDCl₃) δ 8.32(d, J = 8.5 Hz, 1H), 8.21(d, J = 8.5 Hz, 1H), 7.89(dd, J = 8.0, 1.0 Hz, 1H), 7.80(ddd, J = 8.5, 7.0, 1.5 Hz, 1H), 7.66(ddd, J = 8.0, 7.0, 1.0 Hz, 1H), 4.10(s, 3H); ¹³C NMR(125 MHz, CDCl₃) δ 166.0, 147.9, 147.6, 137.4, 130.8, 130.4, 129.4, 128.7, 127.6, 121.1, 53.3; LC-MS (EI⁺) m/z 188.09 [M+H]⁺.

Methyl 5-fluoro-quinoline-2-carboxylate (1b)



5-fluoro-quinoline-2-carboxylic acid was used instead of quinoline-2-carboxylic acid. **1b** (1.65 g, 80.5%). $^1\text{H NMR}$ (500 MHz, CDCl_3) δ 8.59(d, $J = 9.0$ Hz, 1H), 8.25(d, $J = 8.5$ Hz, 1H), 8.13(d, $J = 9.0$ Hz, 1H), 7.75~7.71(m, 1H), 7.34~7.30(m, 1H), 4.11(s, 3H); $^{13}\text{C NMR}$ (125 MHz, CDCl_3) δ 165.58, 157.51(d, $J = 255$ Hz), 148.74, 148.16(d, $J = 2.9$ Hz), 130.79(d, $J = 3.7$ Hz), 129.82(d, $J = 8.5$ Hz), 126.54(d, $J = 4.7$ Hz), 121.08(d, $J = 2.9$ Hz), 120.13(d, $J = 17.1$ Hz), 122.03(d, $J = 18.9$ Hz), 53.29; $^{19}\text{F NMR}$ (282 MHz, CDCl_3) δ -122.42(dd, $J = 9.3, 6.1$ Hz); LC-MS (EI^+) m/z 206.09 $[\text{M}+\text{H}]^+$.

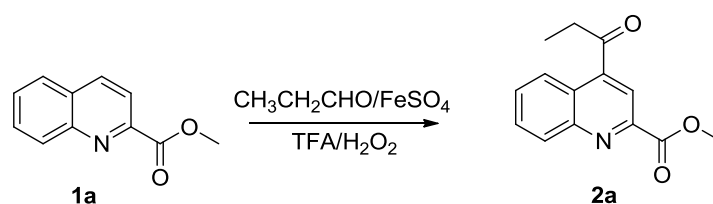
Methyl 6-fluoro-quinoline-2-carboxylate (**1c**)



6-fluoro-quinoline-2-carboxylic acid was used instead of quinoline-2-carboxylic acid. **1c** (1.66 g, 80.9%). $^1\text{H NMR}$ (500 MHz, CDCl_3) δ 8.32(dd, $J = 9.5, 5.5$ Hz, 1H), 8.26(d, $J = 9.0$ Hz, 1H), 8.22(d, $J = 9.0$ Hz, 1H), 7.59~7.55(m, 1H), 7.50(dd, $J = 8.5, 3.0$ Hz, 1H), 4.09(s, 3H); $^{13}\text{C NMR}$ (125 MHz, CDCl_3) δ 165.7, 161.7(d, $J = 251$ Hz), 147.4(d, $J = 2.9$ Hz), 144.6, 136.6(d, $J = 5.6$ Hz), 133.4(d, $J = 9.5$ Hz), 130.2(d, $J = 10.5$ Hz), 121.8, 120.9(d, $J = 25.6$ Hz), 110.6(d, $J = 21.7$ Hz), 53.2; $^{19}\text{F NMR}$ (282 MHz, CDCl_3) δ -109.8(d, $J = 4.7$ Hz); LC-MS (EI^+) m/z 206.08 $[\text{M}+\text{H}]^+$.

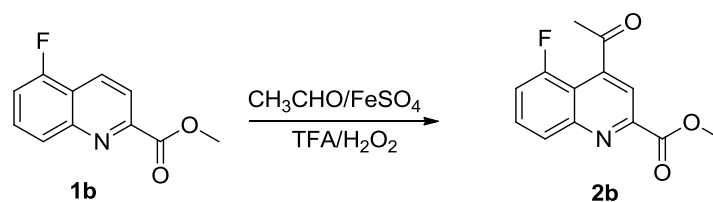
2.1.2. Characterization of methyl 4-acetyl-quinoline-2-carboxylate and its analogues

Methyl 4-propionyl-quinoline-2-carboxylate (**2a**)



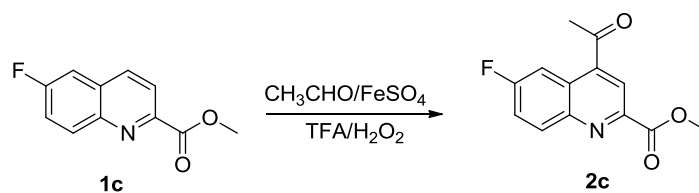
Propionaldehyde was used instead of acetaldehyde. **2z** (1.95 g, 79.9%). ^1H NMR(500 MHz, CDCl_3) δ 8.35~8.33(m, 2H), 7.82(ddd, $J = 8.3, 6.9, 1.4$ Hz, 1H), 7.73~7.70(m, 1H), 4.10(s, 3H), 3.11(q, $J = 5$ Hz, 2 H), 1.29(t, $J = 5$ Hz, 3H); ^{13}C NMR(125 MHz, CDCl_3) δ 203.9, 165.4, 148.5, 147.47, 144.6, 131.1, 130.6, 130.2, 128.7, 125.3, 118.9, 53.4, 35.7, 7.9 ; LC-MS (EI^+) m/z 244.20 $[\text{M}+\text{H}]^+$.

Methyl 4-acetyl-5-fluoro-quinoline-2-carboxylate (**2b**)



2b (2.12 g, 85.9%). ^1H NMR(500 MHz, CDCl_3) δ 8.18(d, $J = 8.5$ Hz, 1H), 8.04(s, 1H), 7.78(tt, $J = 11.3, 5.7$ Hz, 1H), 7.39(ddd, $J = 10.8, 7.8, 0.9$ Hz, 1H), 4.09(s, 3H), 2.66(d, $J = 2.6$ Hz, 3H); ^{13}C NMR(125 MHz, CDCl_3) δ 201.9, 164.8, 156.7(d, $J = 256.0$ Hz), 148.7, 148.5, 146.4, 130.6(d, $J = 9.2$ Hz), 127.3(d, $J = 4.0$ Hz), 117.3, 115.2(d, $J = 14.7$ Hz), 113.8(d, $J = 20.4$ Hz), 53.5, 30.9(d, $J = 7.3$ Hz); ^{19}F NMR(282 MHz, CDCl_3) δ -109.9; LC-MS (EI^+) m/z 248.14 $[\text{M}+\text{H}]^+$.

Methyl 4-acetyl-6-fluoro-quinoline-2-carboxylate (**2c**)



2c (2.05 g, 82.9%). ^1H NMR(500 MHz, CDCl_3) δ 8.50(s, 1H), 8.34(m, 2H), 7.59(m, 1H), 4.10(s, 3H), 2.80(s, 3H); ^{13}C NMR(125 MHz, CDCl_3) δ 199.9, 165.2, 163.4(d, $J = 253.7$ Hz); 147.0(d, $J = 3.2$ Hz), 146.1, 141.9(d, $J = 6.4$ Hz), 133.8(d, $J = 9.8$ Hz), 126.2(d, $J = 11.5$ Hz), 121.4, 121.4(d, $J = 26.1$ Hz), 109.9(d, $J = 25.0$ Hz), 53.6, 29.7; ^{19}F NMR(282 MHz, CDCl_3) δ -106.1(dd, $J = 17.0$, 6.8 Hz); LC-MS (EI^+) m/z 248.12 $[\text{M}+\text{H}]^+$.

2.2 Characterization of TSR derivatives

2.2.1. Characterization of 5'-fluoro-TSR

^1H NMR (400 MHz, CDCl_3 : $\text{CD}_3\text{OD} = 4: 1$): 8.81(s, 1H), 8.33(s, 1H), 8.31(s, 1H), 8.18(s, 1H), 7.63(s, 1H), 7.61(s, 1H), 7.55(s, 1H), 6.73(s, 1H), 6.54(s, 1H), 6.37(m, 1H), 6.25(q, $J = 6.5$ Hz, 1H), 5.97(d, $J = 5.7$ Hz, 1H), 5.85(s, 1H), 5.81(d, $J = 8.8$ Hz, 1H), 5.78(d, $J = 9.6$ Hz, 1H), 5.71(s, 1H), 5.67(q, $J = 7.2$ Hz, 1H), 5.64(s, 1H), 5.39(s, 1H), 5.35(m, 1H), 5.02(dd, $J = 12.1$, 9.6 Hz, 1H), 4.78(q, $J = 6.5$ Hz, 1H), 4.50(m, 1H), 4.46(m, 1H), 4.12(m, 1H), 3.87(q, $J = 6.6$ Hz, 1H), 3.84(q, $J = 6.3$ Hz, 1H), 3.70(m, 1H), 3.68(m, 1H), 3.50(m, 1H), 3.19(t, $J = 12.1$ Hz, 1H), 2.99(m, 1H), 2.96(m, 1H), 2.34(m, 1H), 1.89(m, 1H), 1.74(d, $J = 6.6$ Hz, 3H), 1.69(m, 2H), 1.65(d, $J = 6.5$ Hz, 3H), 1.45(d, $J = 6.5$ Hz, 3H), 1.39(d, $J = 7.5$ Hz, 3H), 1.31(d, $J = 6.3$ Hz, 3H), 1.20(d, $J = 6.6$ Hz, 3H), 1.16(s, 3H), 1.00(d, $J = 6.9$ Hz, 3H), 0.99(m, 1H), 0.92(t, $J = 7.0$ Hz, 3H), 0.85(d, $J = 6.1$ Hz, 3H); ^{13}C NMR (100 MHz, CDCl_3 : $\text{CD}_3\text{OD} = 4: 1$): 173.7, 173.2, 172.0, 170.3, 170.2, 169.8, 169.5, 168.4, 167.7(d, $J = 252.0$ Hz), 166.4, 165.5, 165.4, 162.9, 162.3, 162.2, 162.1, 161.9, 160.5, 159.7, 157.4, 155.4, 152.6, 150.1, 149.9, 146.3, 144.7, 134.7, 134.2, 133.1, 132.1, 128.5, 127.9, 125.7, 125.1, 123.3, 122.5(d, $J = 24.7$ Hz), 118.3, 107.6(d, $J = 19.4$ Hz), 104.6, 103.6, 103.5, 79.0, 77.4, 72.5, 67.9, 67.8, 66.5, 65.8, 65.7, 64.1, 58.3(d, $J = 10.0$ Hz), 57.6, 56.0, 55.9, 52.9, 51.6, 49.2, 38.8, 34.9, 28.3, 24.5, 23.0, 22.8, 19.0, 18.9, 18.8, 18.7, 18.4, 16.0, 15.7, 15.4, 11.5; ^{19}F NMR(282 MHz, CDCl_3 : CD_3OD =4:1) δ -72.97; HRMS (m/z) $[\text{M}+\text{H}]^+$ calcd. For $\text{C}_{72}\text{H}_{85}\text{FN}_{19}\text{O}_{18}\text{S}_5$, 1682.4902; found 1682.4914.

5'-fluoro-TSR shares the overall similarity in spectrum patterns to the parent compound

thiostrepton (Table S2). Analysis of their 1D and 2D NMR spectra revealed the only difference present in the unit **Q**. The new signal of ^{19}F NMR and corresponding changes of the ^1H and ^{13}C NMR signals at Q5, Q6, Q7 and Q10 were observed, indicating that the fluorine atom was successfully introduced into TSR at the expected position.

2.2.2. Characterization of 12'-methyl-TSR

^1H NMR (400 MHz, CDCl_3 : $\text{CD}_3\text{OD} = 4: 1$): 8.83(s, 1H), 8.32(s, 1H), 8.31(s, 1H), 8.22(s, 1H), 7.60(s, 1H), 7.59(s, 1H), 7.31(s, 1H), 7.07(s, 1H), 6.89(d, $J = 9.9$ Hz, 1H), 6.73(d, $J = 2.0$ Hz, 1H), 6.56(s, 1H), 6.38(q, $J = 6.5$ Hz, 1H), 6.37(dd, $J = 9.6, 5.6$ Hz, 1H), 6.24(q, $J = 7.0$ Hz, 1H), 5.84(s, 1H), 5.80(d, $J = 8.8$ Hz, 1H), 5.76(d, $J = 9.6$ Hz, 1H), 5.70(s, 1H), 5.63(d, $J = 2.0$ Hz, 1H), 5.36(s, 1H), 5.32(d, $J = 6.4$ Hz, 1H), 5.06~5.04(m, 1H), 4.96~4.93(m, 1H), 4.74(q, $J = 7.0$ Hz, 1H), 4.47(d, $J = 3.1$ Hz, 1H), 4.43~4.39(m, 1H), 4.10(m, 1H), 3.83(q, $J = 6.5$ Hz, 1H), 3.82~3.80(m, 1H), 3.68(m, 1H), 3.62~3.60(m, 1H), 3.17(t, $J = 12.0$ Hz, 1H), 2.32(m, 1H), 2.96~2.93(m, 2H), 2.98(d, $J = 4.6$ Hz, 1H), 1.92(m, 1H), 1.74(q, $J = 6.6$ Hz, 3H), 1.64~1.60(m, 2H), 1.63(d, $J = 7.0$ Hz, 3H), 1.55~1.53(m, 1H), 1.46(d, $J = 7.0$ Hz, 3H), 1.32(d, $J = 6.6$ Hz, 3H), 1.31(d, $J = 6.6$ Hz, 3H), 1.29(m, 2H), 1.18(s, 3H), 1.10(t, $J = 6.4$ Hz, 3H), 1.00(d, $J = 6.5$ Hz, 3H), 0.90(t, $J = 7.0$ Hz, 3H), 0.85(d, $J = 6.5$ Hz, 3H); ^{13}C NMR (100 MHz, CDCl_3 : $\text{CD}_3\text{OD} = 4: 1$): 174.1, 173.9, 172.6, 170.9, 170.7, 170.2, 169.5, 168.6, 166.9, 166.7, 166.1, 163.4, 162.8, 162.7, 162.6, 162.3, 161.4, 160.3, 157.4, 155.1, 153.8, 150.7, 150.5, 146.9, 144.0, 134.7, 133.4, 132.7, 132.6, 130.2, 129.2, 129.0, 128.5, 128.4, 126.3, 124.5, 123.4, 118.9, 105.0, 104.3, 104.0, 79.5, 77.9, 72.2, 70.2, 68.2, 68.1, 67.0, 66.6, 64.8, 59.5, 58.2, 56.3, 53.6, 52.3, 50.1, 39.0, 35.7, 31.1, 29.3, 23.3, 23.0, 20.3, 19.5, 19.4, 19.3, 16.3, 16.2, 16.0, 12.1, 11.0; HRMS (m/z) $[\text{M}+\text{H}]^+$ calcd. For $\text{C}_{73}\text{H}_{88}\text{N}_{19}\text{O}_{18}\text{S}_5$, 1678.5153; found 1678.5130.

12'-methyl-TSR shares the overall similarity in spectrum patterns to the parent compound thiostrepton (Table S3). Analysis of their 1D and 2D NMR spectra revealed the only difference present in the unit **Q**. The new signal of Q13 and corresponding changes of the ^1H and ^{13}C NMR signals at Q11 and Q12 were observed, indicating that the methyl group was successfully introduced into TSR at the expected position.

2.3. Supplementary Tables

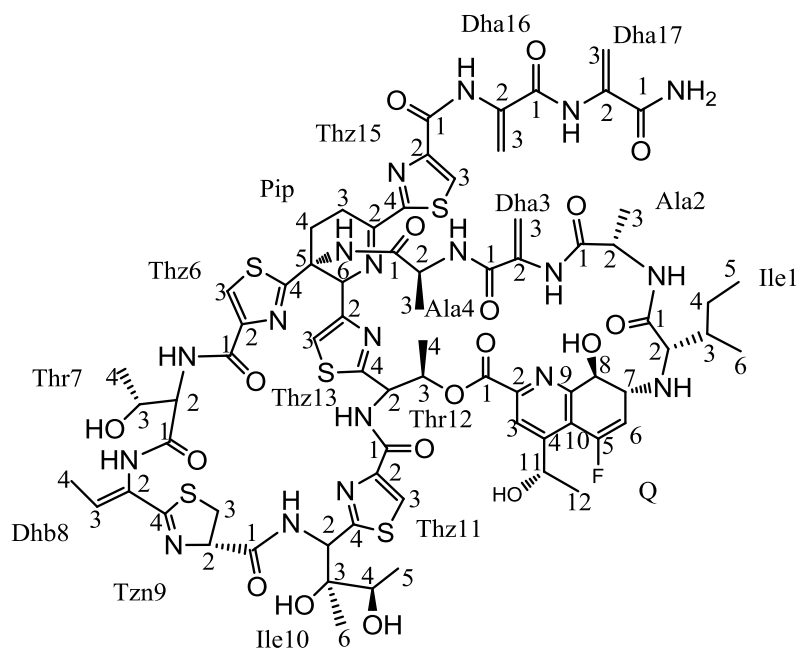
Table S1. Bacteria strains, cell lines and animal models used in this study

	Characteristic(s)	Source / Reference
Strains		
<i>S.laurentii</i> SL1102	TSR non-producing strain, in which the 2-methyltransferase-encoding gene <i>tsrT</i> was inactivated	7
<i>Bacillus subtilis</i> SIPI-JD1001 ^a	Non-drug resistance and for MIC test	8
<i>Staphylococcus aureus</i> SIPI-DJ1002 ^a	Non-drug resistance and for MIC test	8
<i>Staphylococcus aureus</i> ATCC25923 ^a	Non-drug resistance and for MIC test	ATCC
<i>Streptococcus pneumoniae</i> PRSP1063 ^a	Penicillin resistance and for MIC test	Clinical isolates ^c
<i>Streptococcus pneumoniae</i> PRSP2831 ^a	Penicillin resistance and for MIC test	Clinical isolates ^c
<i>Streptococcus pneumoniae</i> ^a PRSP224588	Penicillin resistance and for MIC test	Clinical isolates ^c
<i>Staphylococcus aureus</i> MRSA-s1 ^a	Methicillin resistance and for MIC test	Clinical isolates ^c
<i>Staphylococcus aureus</i> MRSA-SAU3 ^a	Methicillin resistance and for MIC test	Clinical isolates ^c
<i>Staphylococcus aureus</i> MRSA-SAU5 ^a	Methicillin resistance and for MIC test	Clinical isolates ^c
<i>Enterococcus faecium</i>	Vancomycin resistance and for MIC	Clinical isolates ^c

VRE3 ^a	test	
<i>Enterococcus faecium</i>	Vancomycin resistance and for MIC	Clinical isolates ^c
VRE73 ^a	test	
<i>Enterococcus faecium</i>	Vancomycin resistance and for MIC	Clinical isolates ^c
VRE83 ^a	test	
<i>Acinetobacter baumannii</i>	Colistin resistance and for MIC test	Developed in this study
Azj06-200 ^b		
<i>Acinetobacter junii</i>	Colistin resistance and for MIC test	Clinical isolates ^c
A 1322 ^b		
<i>Chryseobacterium meningosepticum</i>	Colistin resistance and for MIC test	Clinical isolates ^c
A 2757 ^b		

^a Gram-positive bacterium; ^b Gram-negative bacterium; ^c Samples of clinical pathogenic bacteria were selected and stored in Department of Infectious Diseases, Sir Run Run Shaw Hospital, College of Medicine, Zhejiang University.

Table S2. ^1H and ^{13}C NMR assignments of **5'-fluoro-TSR**



5-F-TSR			TSR ¹⁰		
Position	$\Delta\epsilon$ [ppm] (mult, <i>J</i> in Hz)	δ_{H} [ppm] (mult, <i>J</i> in Hz)	Position	δ_{C} [ppm] (mult, <i>J</i> in Hz)	δ_{H} [ppm] (mult, <i>J</i> in Hz)
<i>Ile1</i>			<i>Ile1</i>		
Ile1-1	173.7; C _q		Ile1-1	173.7; C _q	
Ile1-2	65.8; CH	2.99(m)	Ile1-2	65.6; CH	2.81(d, 4.6)
Ile1-3	38.8; CH	1.89(m)	Ile1-3	38.5; CH	1.69(m)
Ile1-4	22.8; CH ₂	1.69(m) 0.99(m)	Ile1-4	24.6; CH ₂	1.21(m) 0.95(m)
Ile1-5	11.5; CH ₃	0.92(t, 7.0)	Ile1-5	11.3; CH ₃	0.74(t, 7.1)
Ile1-6	15.7; CH ₃	1.00(d, 6.9)	Ile1-6	15.5; CH ₃	0.82(d, 6.9)
<i>Ala2</i>			<i>Ala2</i>		
Ala2-1	170.3; C _q		Ala2-1	168.8; C _q	
Ala2-2	49.2; CH	3.87(q, 6.6)	Ala2-2	49.4; CH	3.67(dq, 5.4,6.8)

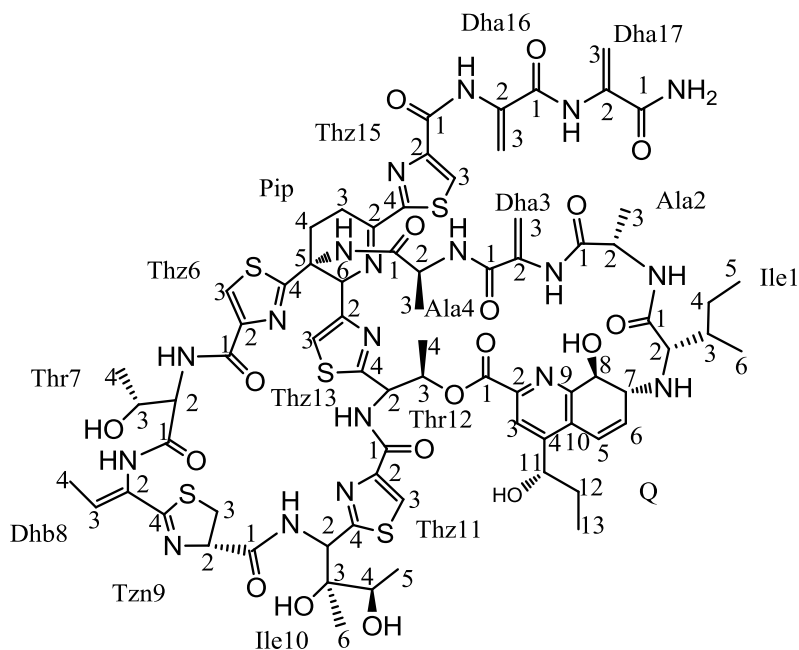
Ala2-3	19.0; CH ₃	1.20(d, 6.6)	Ala2-3	18.9; CH ₃	1.03(d, 6.8)
<i>Dha3</i>			<i>Dha3</i>		
Dha3-1	162.9; Cq		Dha3-1	162.9; Cq	
Dha3-2	132.1; Cq		Dha3-2	132.3; Cq	
Dha3-3	103.5; CH ₂	5.85(s) 5.39(s)	Dha3-3	102.8; CH ₂	5.66(d, 1.92) 5.19(s)
<i>Ala4</i>			<i>Ala4</i>		
Ala4-1	173.2; Cq		Ala4-1	173.3; Cq	
Ala4-2	51.6; CH	4.78(q, 6.5)	Ala4-2	51.9; CH	4.59(dq, 6.5, 7.8)
Ala4-3	18.8; CH ₃	1.45(d, 6.5)	Ala4-3	18.8; CH ₃	1.28(d, 6.6)
<i>Pip</i>			<i>Pip</i>		
Pip-2	161.9; Cq		Pip-2	161.9; Cq	
Pip-3	24.5; CH ₂	3.50(m) 2.96(m)	Pip-3	24.6; CH ₂	3.32(m) 2.76(m)
Pip-4	28.3; CH ₂	4.12(m) 2.34(m)	Pip-4	29.2; CH ₂	3.92(m) 2.16(m)
Pip-5	57.6; Cq		Pip-5	57.6; Cq	
Pip-6	64.1; CH	5.35(m)	Pip-6	64.2; CH	5.16(s, br)
<i>Thz6</i>					
Thz6-1	162.1; Cq		Thz6-1	161.7; Cq	
Thz6-2	146.3; Cq		Thz6-2	146.4; Cq	
Thz6-3	125.1; CH	8.18(s)	Thz6-3	124.9; CH	8.01(s)
Thz6-4	169.5; Cq		Thz6-4	169.7; Cq	
<i>Thr7</i>			<i>Thr7</i>		
Thr7-1	165.5; Cq		Thr7-1	165.5; Cq	
Thr7-2	56.0; CH	4.46(m)	Thr7-2	55.6; CH	4.27(dd, 3.2, 7.6)
Thr7-3	66.5; CH	1.69(m)	Thr7-3	66.5; CH	1.35(m)

Thr7-4	18.7; CH ₃	0.85(d, 6.1)	Thr7-4	18.9; CH ₃	1.56(d, 6.5)
<i>Dhb8</i>			<i>Dhb8</i>		
Dhb8-2	128.5; Cq		Dhb8-2	128.4; Cq	
Dhb8-3	133.1; CH	6.25(q, 6.5)	Dhb8-3	132.5; CH	6.07(q, 7.1)
Dhb8-4	15.4; CH ₃	1.65(d, 6.5)	Dhb8-4	15.2; CH ₃	1.46(d, 7.0)
<i>Tzn9</i>			<i>Tzn9</i>		
Tzn9-1	172.0; Cq		Tzn9-1	171.9; Cq	
Tzn9-2	79.0; CH	5.02(dd, 12.1, 9.6)	Tzn9-2	78.9; CH	4.83(dd, 9.6, 12.6)
Tzn9-3	34.9; CH ₂	3.70(m) 3.19(t, 12.1)	Tzn9-3	34.8; CH ₂	3.51(dd, 9.0, 11.5)
Tzn9-4	170.2; Cq		Tzn9-4	170.2; Cq	
<i>Ile10</i>			<i>Ile10</i>		
Ile10-2	52.9; CH	5.78(d, 9.6)	Ile10-2	53.1; CH	5.62(d, 9.9)
Ile10-3	77.4; Cq		Ile10-3	77.2; Cq	
Ile10-4	67.8; CH	3.84(q, 6.3)	Ile10-4	67.7; CH	3.67(d, 6.5)
Ile10-5	16.0; CH ₃	1.31(d, 6.3)	Ile10-5	15.9; CH ₃	1.15(d, 6.6)
Ile10-5	18.4; CH ₃	1.16(s)	Ile10-5	18.3; CH ₃	0.99(s)
<i>Thz11</i>			<i>Thz11</i>		
Thz11-1	162.2; Cq		Thz11-1	162.1; Cq	
Thz11-2	150.1; Cq		Thz11-2	150.9; Cq	
Thz11-3	125.7; CH	8.31(s)	Thz11-3	125.4; CH	8.13(s)
Thz11-4	166.4; Cq		Thz11-4	166.3; Cq	
<i>Thr12</i>			<i>Thr12</i>		
Thr12-2	55.9; CH	5.81(d, 8.8)	Thr12-2	55.8; CH	5.62(d, 7.6)
Thr12-3	72.5; CH	6.37(m)	Thr12-3	72.0; CH	6.19(m)
Thr12-4	18.9; CH ₃	1.74(d, 6.6)	Thr12-4	18.7; CH ₃	1.56(d, 6.5)
<i>Thz13</i>			<i>Thz13</i>		
Thz13-2	157.9; Cq		Thz13-2	157.2; Cq	

Thz13-3	118.3; CH	7.61(s)	Thz13-3	118.2; CH	7.40(s)
Thz13-4	169.8; Cq		Thz13-4	169.9; Cq	
<i>Thz15</i>			<i>Thz15</i>		
Thz15-1	159.7; Cq		Thz15-1	159.6; Cq	
Thz15-2	149.9; Cq		Thz15-2	149.9; Cq	
Thz15-3	127.9; CH	8.33(s)	Thz15-3	127.6; CH	8.14(s)
ThZ15-4	168.4; Cq		ThZ15-4	168.4; Cq	
<i>Dha16</i>			<i>Dha16</i>		
Dha16-1	162.3; Cq		Dha16-1	162.0; Cq	
Dha16-2	134.2; Cq		Dha16-2	134.2; Cq	
Dha16-3	103.6; CH ₂	6.73(s) 5.64(s)	Dha16-3	103.3; CH ₂	6.54(d, 1.9) 5.48(d, 1.9)
<i>Dha17</i>			<i>Dha17</i>		
Dha17-1	165.4; Cq		Dha17-1	165.9; Cq	
Dha17-2	134.7; Cq		Dha17-2	133.0; Cq	
Dha17-3	104.6;CH ₂	6.54(s) 5.71(s)	Dha17-3	104.3;CH ₂	6.37(d, 1.2) 5.52(d, 1.2)
<i>Q</i>			<i>Q</i>		
Q-1	160.5; Cq		Q-1	160.8; Cq	
Q-2	144.7; Cq		Q-2	143.6; Cq	
Q-3	123.3; CH	7.55(s)	Q-3	122.3; CH	7.13(s)
Q-4	155.4; Cq		Q-4	153.4; Cq	
<i>Q-5</i>	<i>167.7; CF(d, 252.0)</i>		<i>Q-5</i>	<i>123.2; CH</i>	<i>6.73(d, 10.1)</i>
<i>Q-6</i>	<i>107.6; CH(d, 19.4)</i>	<i>5.97(d, 5.7)</i>	<i>Q-6</i>	<i>129.9; CH</i>	<i>6.23(dd, 5.6, 9.9)</i>
<i>Q-7</i>	<i>58.3; CH(d, 10.0)</i>	<i>3.68(m)</i>	<i>Q-7</i>	<i>59.0; CH</i>	<i>3.46(dd, 1.7, 5.5)</i>
Q-8	67.9; CH	4.50(m)	Q-8	67.3; CH	4.32(d, 1.8)

Q-9	152.6; Cq		Q-9	154.5; Cq	
Q-10	122.5; Cq(d, 24.7)		Q-10	127.2; Cq	
Q-11	65.7; CH	5.67(q, 7.2)	Q-11	64.4; CH	5.16(q, 6.4)
Q-12	23.0; CH ₃	1.39(d, 7.5)	Q-12	22.5; CH ₃	1.21(d, 6.6)

Table S3. ^1H and ^{13}C NMR assignments of **12'-methyl-TSR**



Bing-TSR			TSR ¹⁰		
Position	$\Delta\epsilon$ [ppm] (mult, <i>J</i> in Hz)	δ_{H} [ppm] (mult, <i>J</i> in Hz)	Position	δ_{C} [ppm] (mult, <i>J</i> in Hz)	δ_{H} [ppm] (mult, <i>J</i> in Hz)
<i>Ile1</i>			<i>Ile1</i>		
Ile1-1	174.1; C _q		Ile1-1	173.7; C _q	
Ile1-2	66.6; CH	2.98(d, 4.6)	Ile1-2	65.6; CH	2.81(d, 4.6)
Ile1-3	39.0; CH	1.92(m)	Ile1-3	38.5; CH	1.69(m)
Ile1-4	23.3; CH ₂	1.29(m)	Ile1-4	24.6; CH ₂	1.21(m) 0.95(m)
Ile1-5	12.1; CH ₃	0.90(t, 7.0)	Ile1-5	11.3; CH ₃	0.74(t, 7.1)
Ile1-6	16.2; CH ₃	1.00(d, 6.5)	Ile1-6	15.5; CH ₃	0.82(d, 6.9)
<i>Ala2</i>			<i>Ala2</i>		
Ala2-1	173.9; C _q		Ala2-1	168.8; C _q	
Ala2-2	50.1; CH	3.83(q, 6.5)	Ala2-2	49.4; CH	3.67(dq, 5.4,6.8)

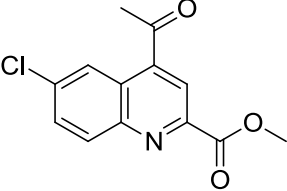
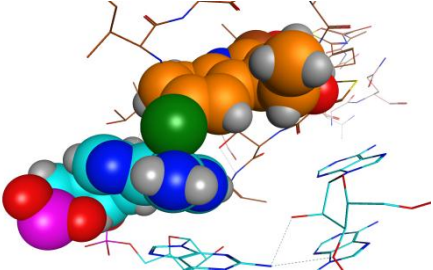
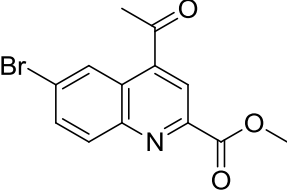
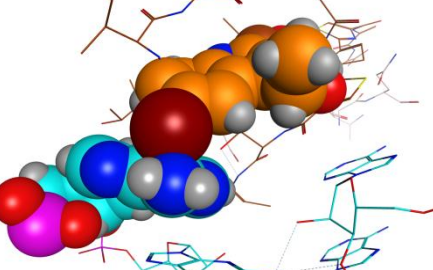
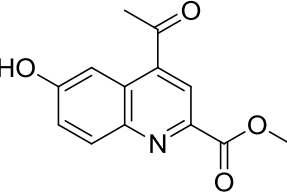
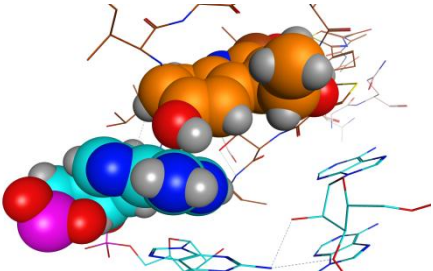
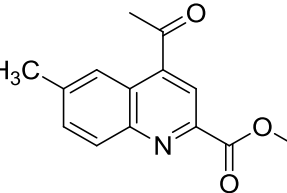
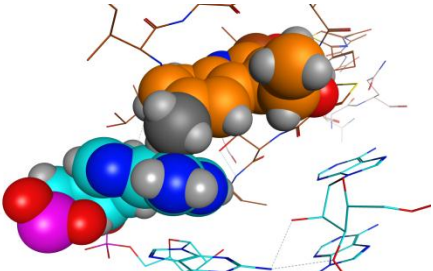
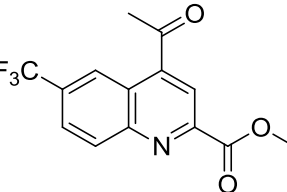
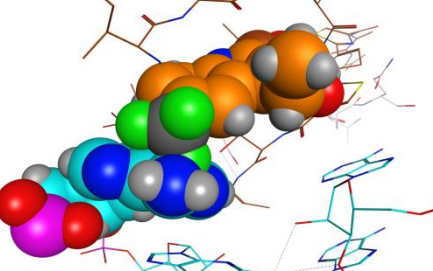
Ala2-3	16.2; CH ₃	1.32(d, 6.6)	Ala2-3	18.9; CH ₃	1.03(d, 6.8)
<i>Dha3</i>			<i>Dha3</i>		
Dha3-1	163.4; Cq		Dha3-1	162.9; Cq	
Dha3-2	134.7; Cq		Dha3-2	132.3; Cq	
Dha3-3	104.3; CH ₂	5.84(s) 5.36(s)	Dha3-3	102.8; CH ₂	5.66(d, 1.92) 5.19(s)
<i>Ala4</i>			<i>Ala4</i>		
Ala4-1	172.6; Cq		Ala4-1	173.3; Cq	
Ala4-2	52.3; CH	4.74(q, 7.0)	Ala4-2	51.9; CH	4.59(dq, 6.5, 7.8)
Ala4-3	20.3; CH ₃	1.46(d, 7.0)	Ala4-3	18.8; CH ₃	1.28(d, 6.6)
<i>Pip</i>			<i>Pip</i>		
Pip-2	162.8; Cq		Pip-2	161.9; Cq	
Pip-3	23.0; CH ₂	2.96~2.93(m)	Pip-3	24.6; CH ₂	3.32(m) 2.76(m)
Pip-4	29.3; CH ₂	4.10(m) 2.32(m)	Pip-4	29.2; CH ₂	3.92(m) 2.16(m)
Pip-5	58.2; Cq		Pip-5	57.6; Cq	
Pip-6	64.8; CH	5.32(d, 6.4)	Pip-6	64.2; CH	5.16(s, br)
<i>Thz6</i>					
Thz6-1	162.3; Cq		Thz6-1	161.7; Cq	
Thz6-2	146.9; Cq		Thz6-2	146.4; Cq	
Thz6-3	128.4; CH	8.32(s)	Thz6-3	124.9; CH	8.01(s)
Thz6-4	170.2; Cq		Thz6-4	169.7; Cq	
<i>Thr7</i>			<i>Thr7</i>		
Thr7-1	166.1; Cq		Thr7-1	165.5; Cq	
Thr7-2	56.3; CH	4.47(d,3.1)	Thr7-2	55.6; CH	4.27(dd, 3.2, 7.6)
Thr7-3	67.0; CH	1.55~1.53(m)	Thr7-3	66.5; CH	1.35(m)

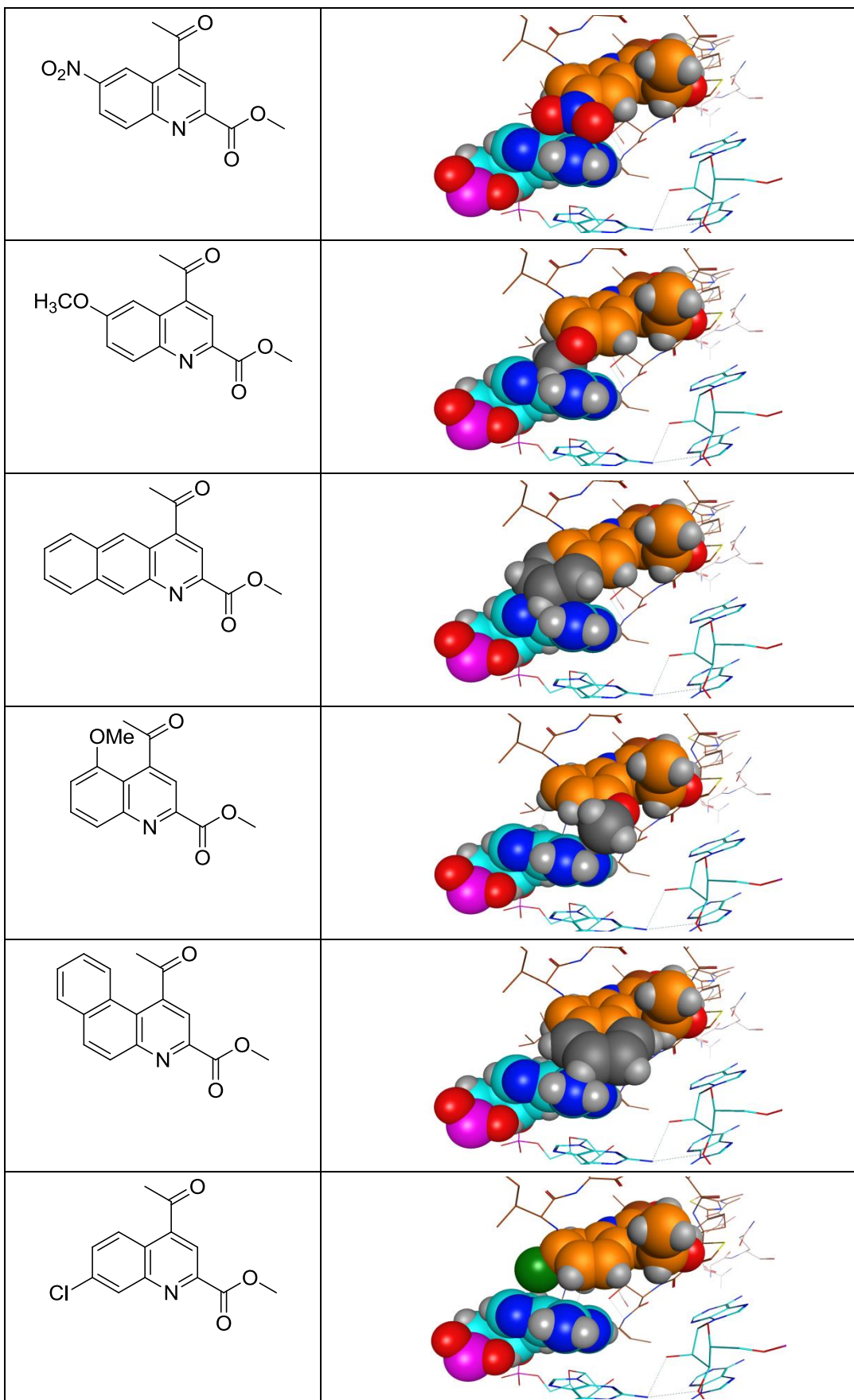
Thr7-4	19.5; CH ₃	0.85(d, 6.5)	Thr7-4	18.9; CH ₃	1.56(d, 6.5)
<i>Dhb8</i>			<i>Dhb8</i>		
Dhb8-2	129.0; Cq		Dhb8-2	128.4; Cq	
Dhb8-3	133.4; CH	6.24(q, 7.0)	Dhb8-3	132.5; CH	6.07(q, 7.1)
Dhb8-4	16.0; CH ₃	1.63(d, 67.0)	Dhb8-4	15.2; CH ₃	1.46(d, 7.0)
<i>Tzn9</i>			<i>Tzn9</i>		
Tzn9-1	170.9; Cq		Tzn9-1	171.9; Cq	
Tzn9-2	79.5; CH	4.96~4.93(m)	Tzn9-2	78.9; CH	4.83(dd, 9.6, 12.6)
Tzn9-3	35.7; CH ₂	3.68(m) 3.17(t, 12.0)	Tzn9-3	34.8; CH ₂	3.51(dd, 9.0, 11.5)
Tzn9-4	170.7; Cq		Tzn9-4	170.2; Cq	
<i>Ile10</i>			<i>Ile10</i>		
Ile10-2	53.6; CH	5.76(d, 9.6)	Ile10-2	53.1; CH	5.62(d, 9.9)
Ile10-3	77.9; Cq		Ile10-3	77.2; Cq	
Ile10-4	68.2; CH	3.82~3.80(m)	Ile10-4	67.7; CH	3.67(d, 6.5)
Ile10-5	16.3; CH ₃	1.31(d, 6.6)	Ile10-5	15.9; CH ₃	1.15(d, 6.6)
Ile10-5	19.4; CH ₃	1.18(s)	Ile10-5	18.3; CH ₃	0.99(s)
<i>Thz11</i>			<i>Thz11</i>		
Thz11-1	162.7; Cq		Thz11-1	162.1; Cq	
Thz11-2	150.5; Cq		Thz11-2	150.9; Cq	
Thz11-3	126.3; CH	8.31(s)	Thz11-3	125.4; CH	8.13(s)
Thz11-4	166.7; Cq		Thz11-4	166.3; Cq	
<i>Thr12</i>			<i>Thr12</i>		
Thr12-2	56.3; CH	5.80(d, 8.8)	Thr12-2	55.8; CH	5.62(d, 7.6)
Thr12-3	72.2; CH	6.38(q, 6.5))	Thr12-3	72.0; CH	6.19(m)
Thr12-4	19.3; CH ₃	1.74(d, 6.6)	Thr12-4	18.7; CH ₃	1.56(d, 6.5)
<i>Thz13</i>			<i>Thz13</i>		
Thz13-2	157.4; Cq		Thz13-2	157.2; Cq	

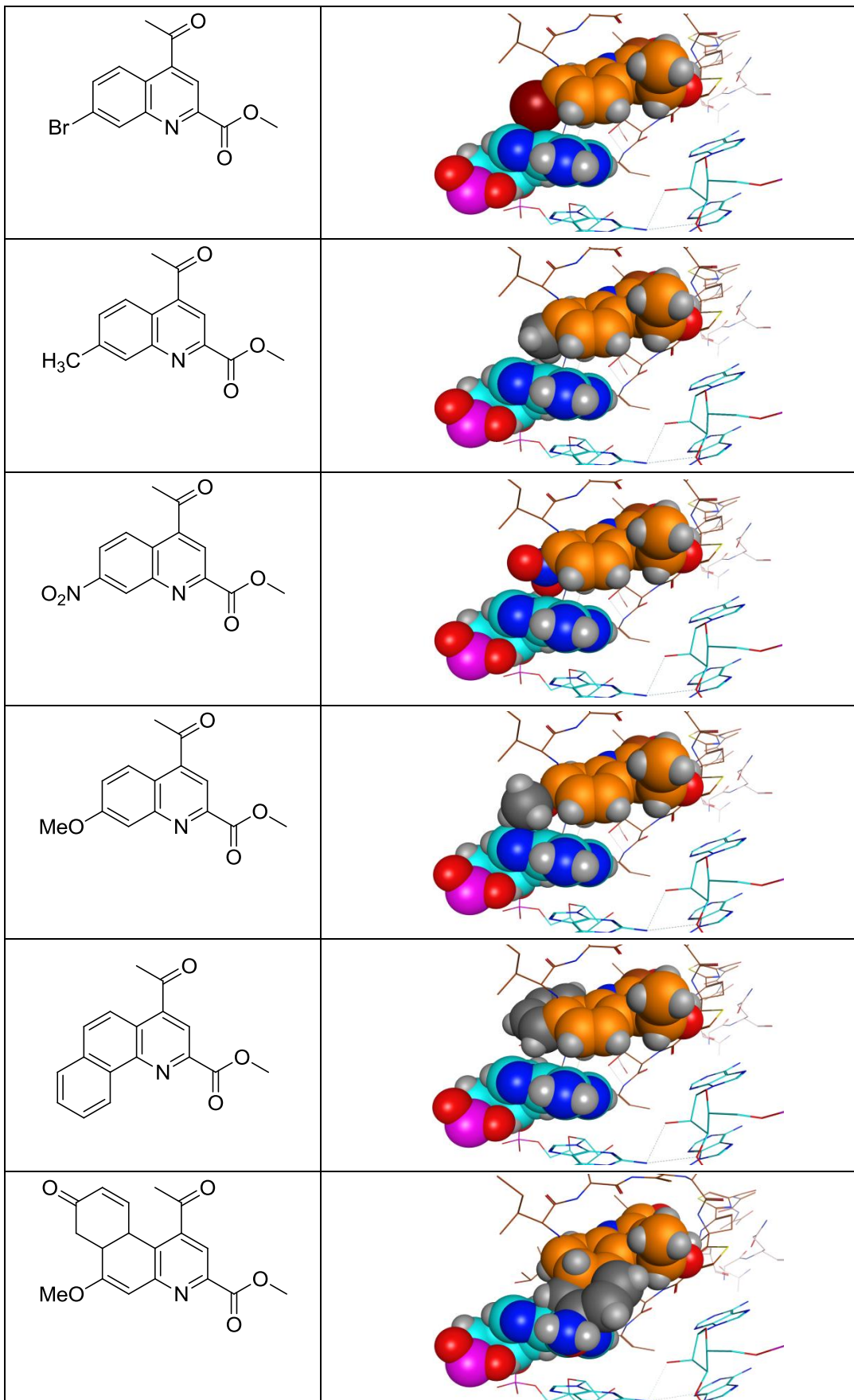
Thz13-3	118.9; CH	7.59(s)	Thz13-3	118.2; CH	7.40(s)
Thz13-4	169.5; Cq		Thz13-4	169.9; Cq	
<i>Thz15</i>			<i>Thz15</i>		
Thz15-1	160.3; Cq		Thz15-1	159.6; Cq	
Thz15-2	150.7; Cq		Thz15-2	149.9; Cq	
Thz15-3	125.8; CH	8.22(s)	Thz15-3	127.6; CH	8.14(s)
Thz15-4	168.6; Cq		Thz15-4	168.4; Cq	
<i>Dha16</i>			<i>Dha16</i>		
Dha16-1	162.6; Cq		Dha16-1	162.0; Cq	
Dha16-2	132.7; Cq		Dha16-2	134.2; Cq	
Dha16-3	104.0; CH ₂	6.73(d, 2.0) 5.63(d, 2.0)	Dha16-3	103.3; CH ₂	6.54(d, 1.9) 5.48(d, 1.9)
<i>Dha17</i>			<i>Dha17</i>		
Dha17-1	166.9; Cq		Dha17-1	165.9; Cq	
Dha17-2	132.6; Cq		Dha17-2	133.0; Cq	
Dha17-3	105.0; CH ₂	6.56(s) 5.70(s)	Dha17-3	104.3; CH ₂	6.37(d, 1.2) 5.52(d, 1.2)
<i>Q</i>			<i>Q</i>		
Q-1	161.4; Cq		Q-1	160.8; Cq	
Q-2	144.0; Cq		Q-2	143.6; Cq	
Q-3	123.4; CH	7.31(s)	Q-3	122.3; CH	7.13(s)
Q-4	153.8; Cq		Q-4	153.4; Cq	
Q-5	124.5; CH	6.89(d, 9.9)	Q-5	123.2; CH	6.73(d, 10.1)
Q-6	130.2; CH	6.37(dd, 5.6, 9.6)	Q-6	129.9; CH	6.23(dd, 5.6, 9.9)
Q-7	59.5; CH	3.62~3.60(m)	Q-7	59.0; CH	3.46(dd, 1.7, 5.5)
Q-8	68.1; CH	4.43~4.39(m)	Q-8	67.3; CH	4.32(d, 1.8)
Q-9	155.1; Cq		Q-9	154.5; Cq	

Q-10	129.2; Cq		Q-10	127.2; Cq	
Q-11	70.2; CH	5.06~5.04(m)	Q-11	64.4; CH	5.16(q, 6.4)
Q-12	31.1; CH ₂	1.64~1.60(m)	Q-12	22.5; CH ₃	1.21(d, 6.6)
Q-13	11.0; CH ₃	1.10(t, 6.4)			

Table S4. The in silico screen and molecular modeling of the interaction between modified QA moiety and A1067

Modified QA precursors	Destroyed interactions between QA and A1067
	
	
	
	
	





2.4. Supplementary Figures

Fig. S1 The isocontour plot in mesh of $\Delta\rho_{\text{QA-A}} = \rho_{\text{QA-A}} - \rho_{\text{QA}} - \rho_{\text{A}}$ for TSR. The isovalue was set to 0.0004. Purple=0.0004 au, cyan=-0.0004 au. The purple mesh in the figure indicates that the electron density increases in the complex, while the cyan mesh shows that the electron density decreases. An obvious $\Delta\rho$ difference could be observed near the double bond of QA. The ρ of the part of the double bond in QA near to adenine decreases obviously, while the ρ of the corresponding part in adenine increases, implying that a π - π interaction between QA and adenine may exist.

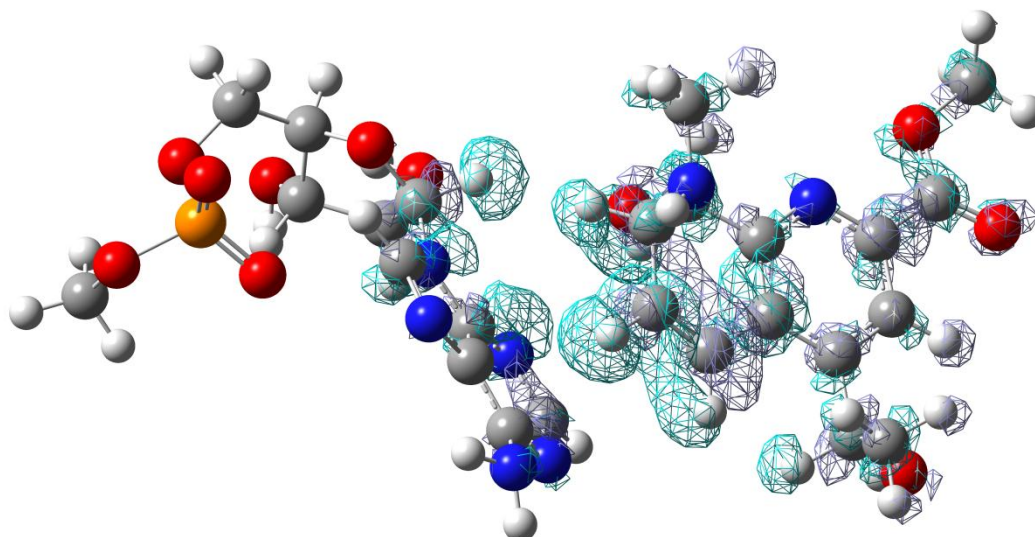


Fig. S2 The two-layer model for TSR (applicable to its derivatives) optimization in Gaussian. The high layer is shown in the ball-stick mode, while the low layer is in wireframe mode.

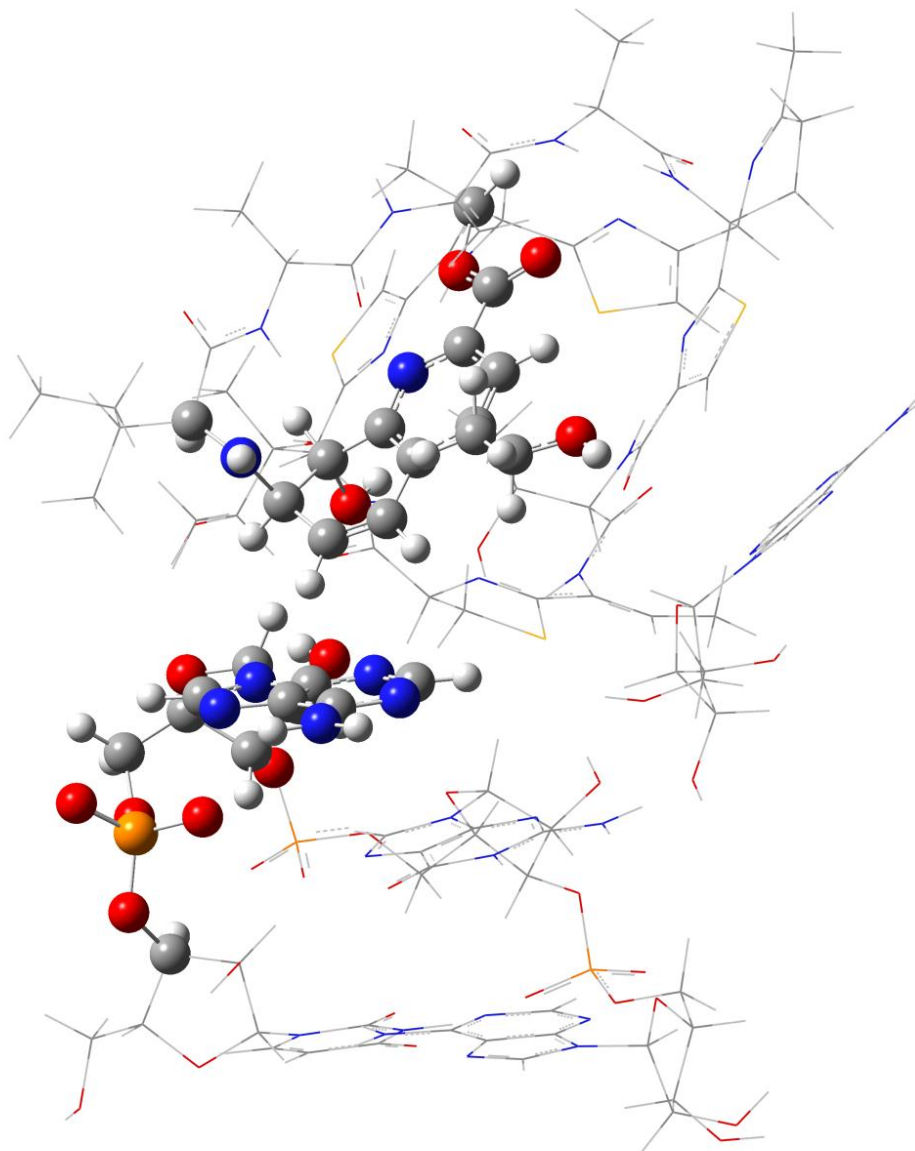


Fig. S3 Proposed biosynthetic pathway for QA formation and incorporation

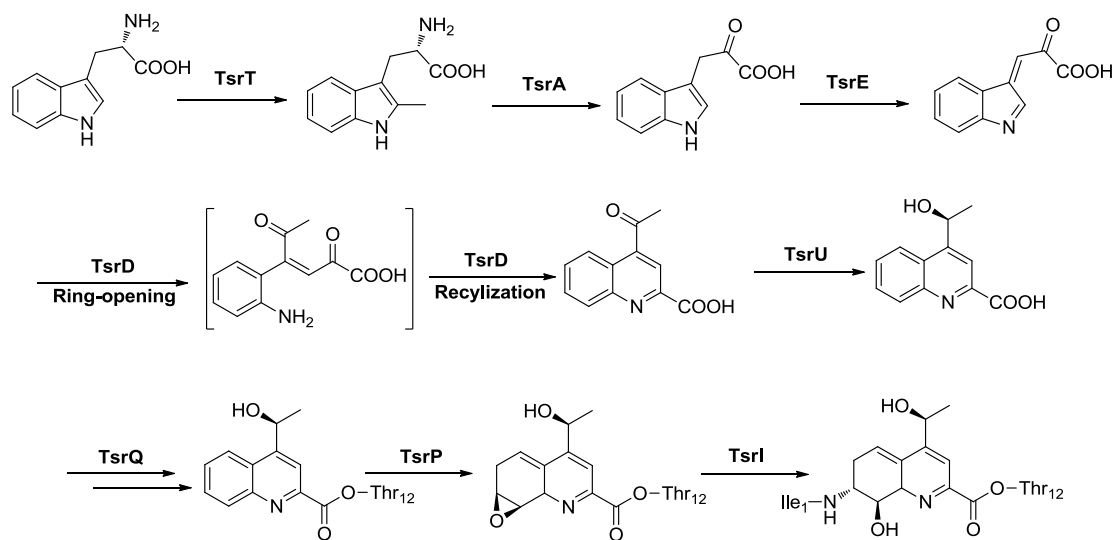
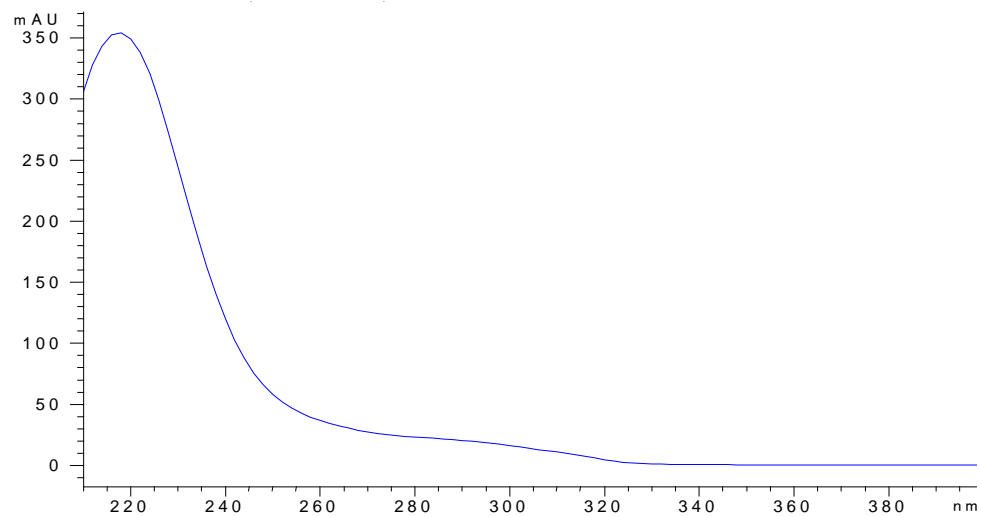


Fig. S4 Ultraviolet absorption of 5'-fluoro-TSR (A) and 12'-methyl-TSR (B)

A.



B.

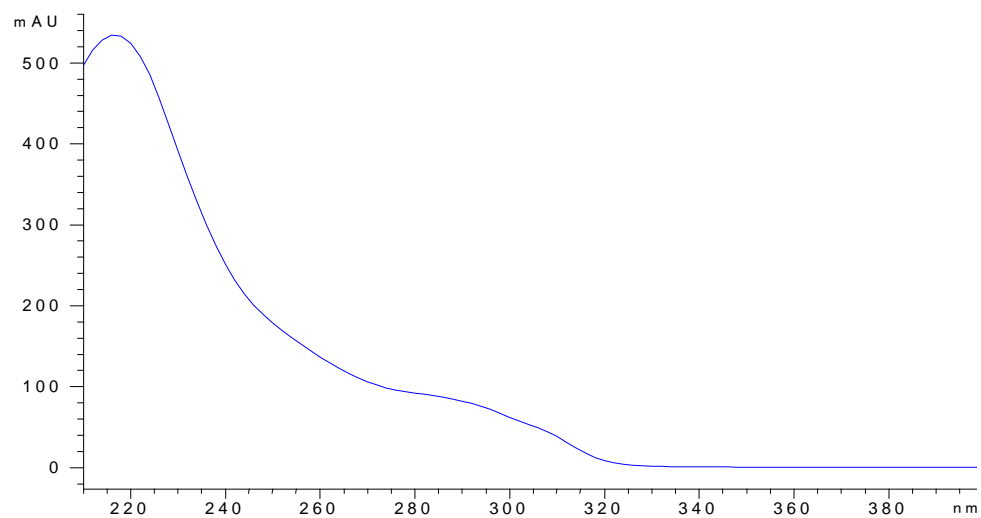
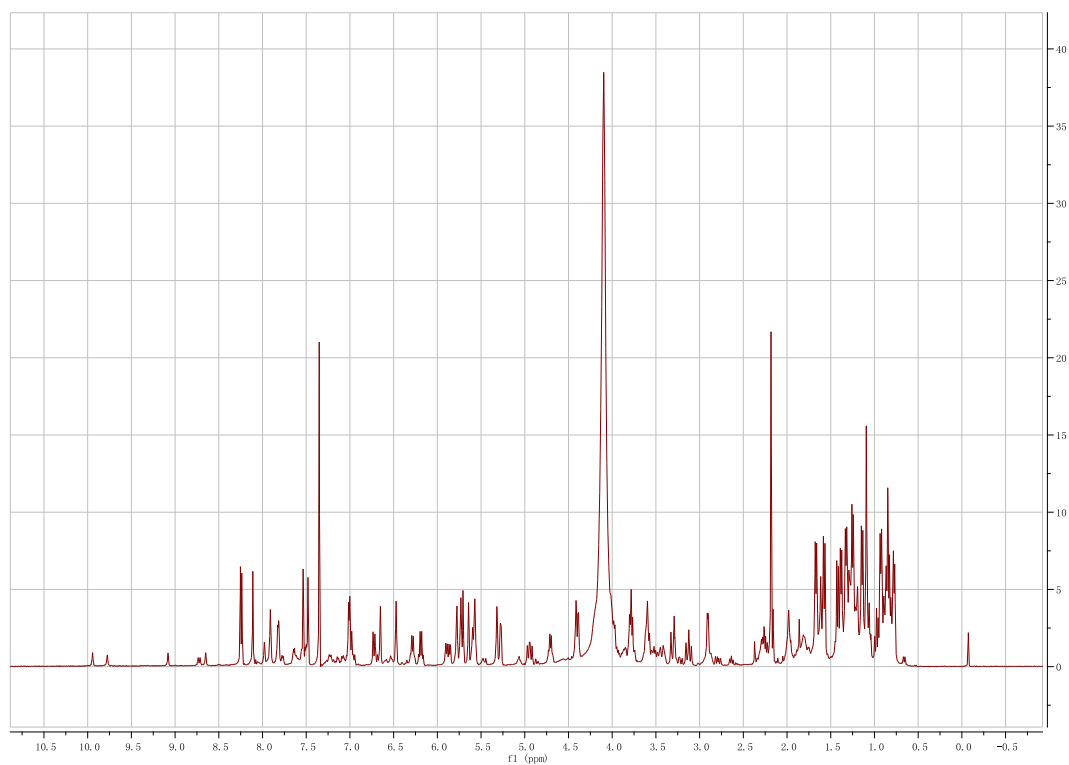
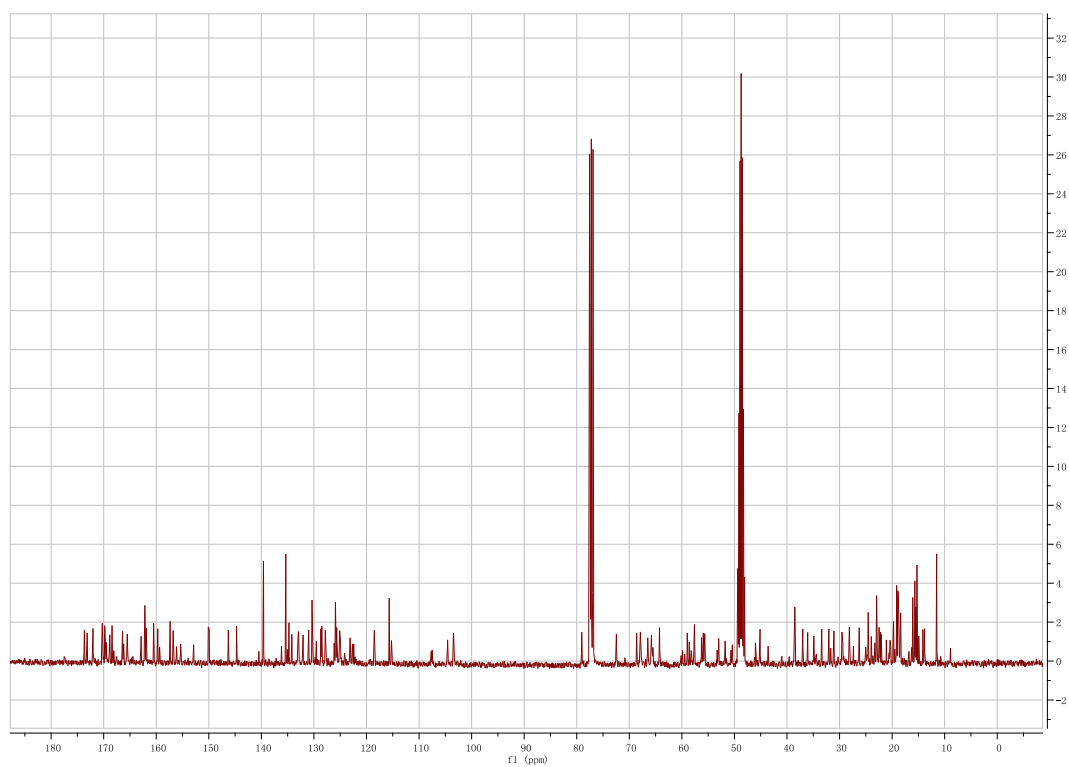


Fig. S5 1D and 2D NMR spectra of 5'-fluoro-TSR

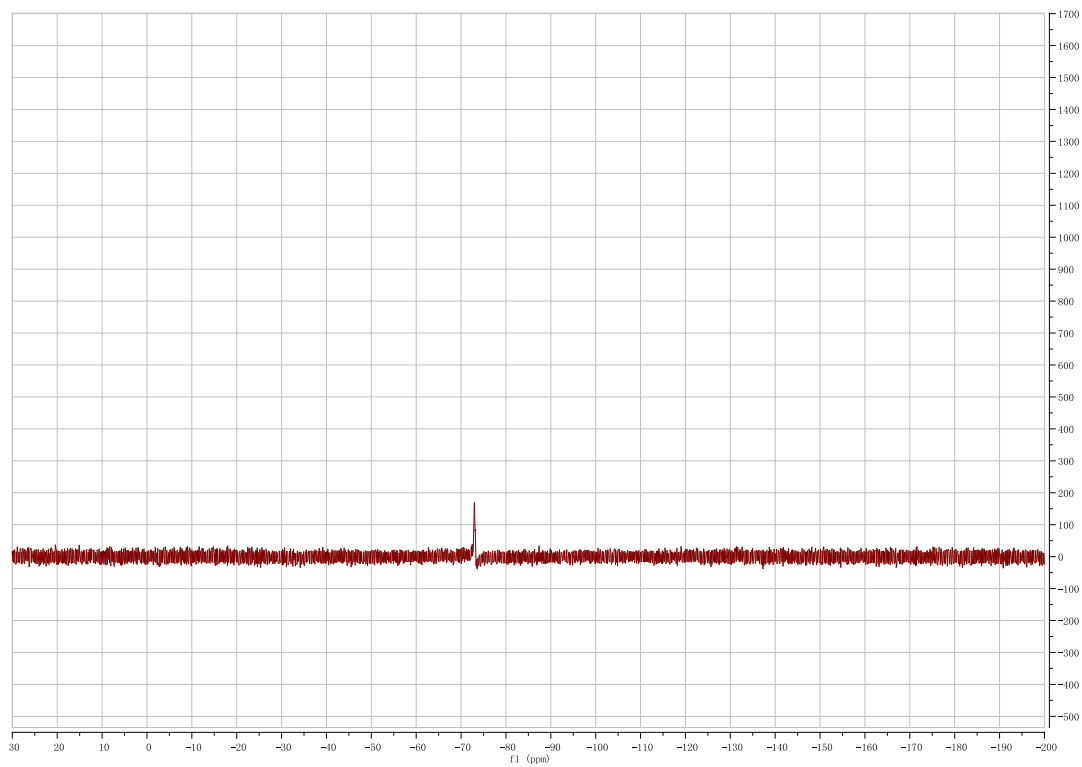
^1H NMR (400 MHz, $\text{CDCl}_3:\text{CD}_3\text{OD} = 4:1$)



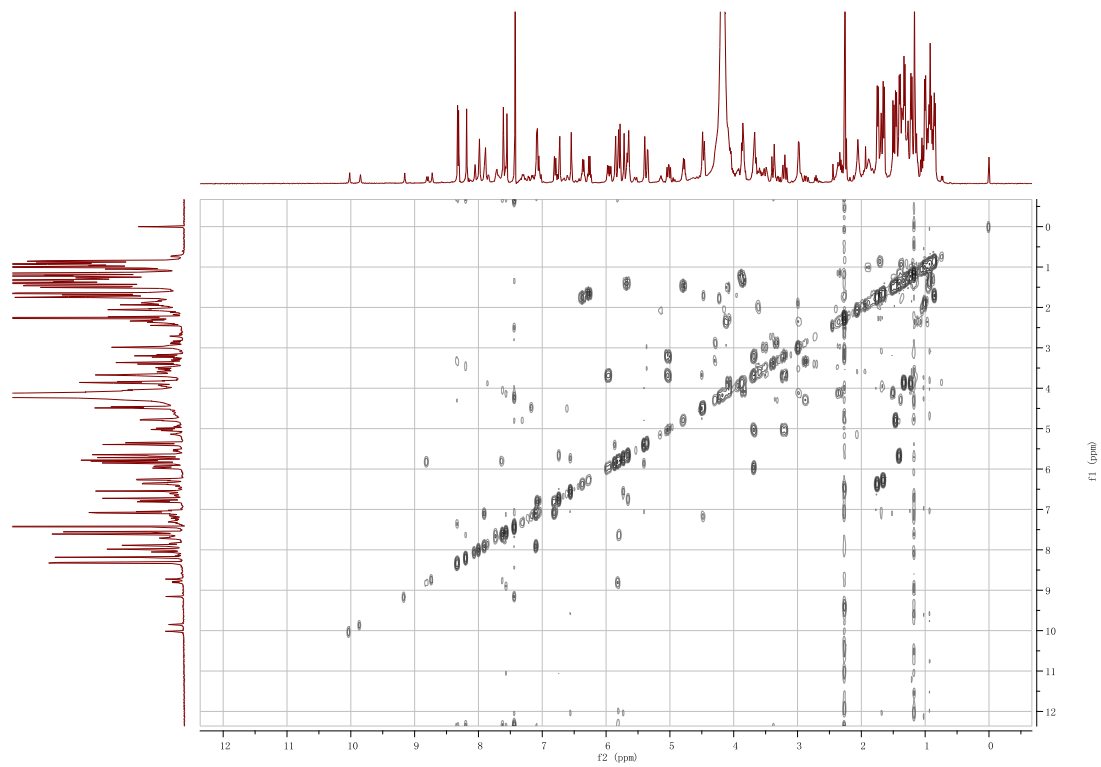
^{13}C NMR (100 MHz, $\text{CDCl}_3:\text{CD}_3\text{OD} = 4:1$)



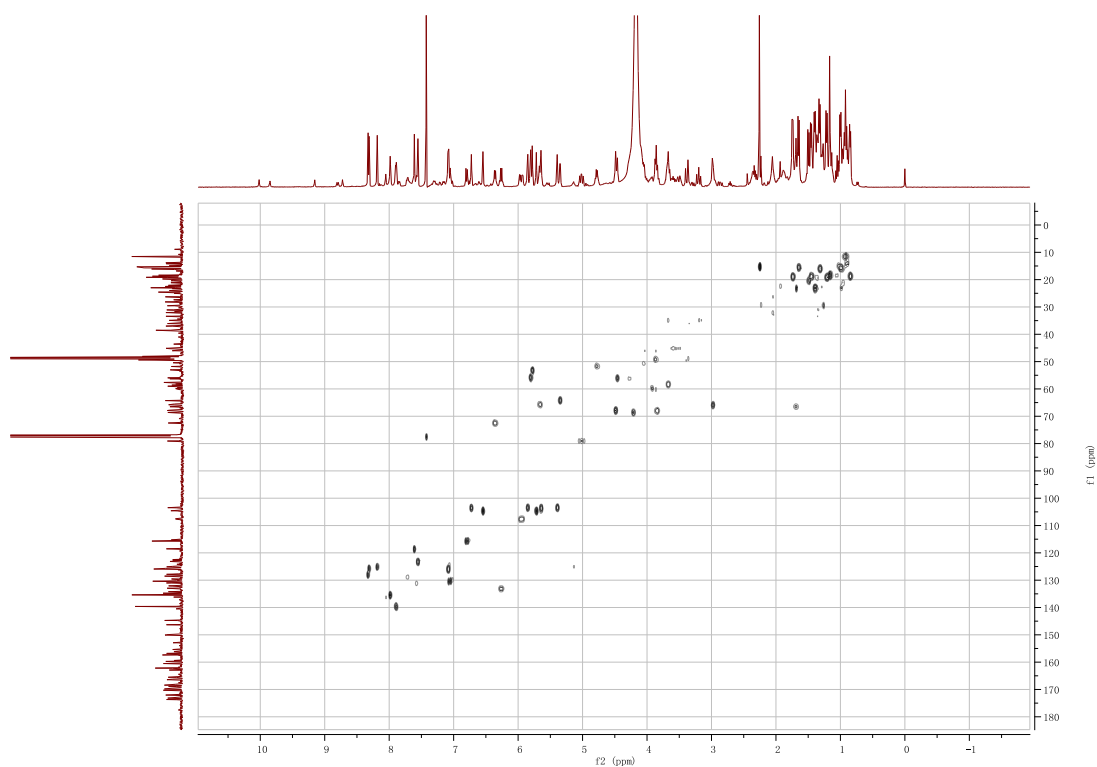
¹⁹F NMR (282 MHz, CDCl₃:CD₃OD = 4:1)



gCOSY (400 MHz, CDCl₃:CD₃OD = 4:1)



gHMQC (400 MHz, CDCl₃:CD₃OD = 4:1)



gHMBC (400 MHz, CDCl₃:CD₃OD = 4:1)

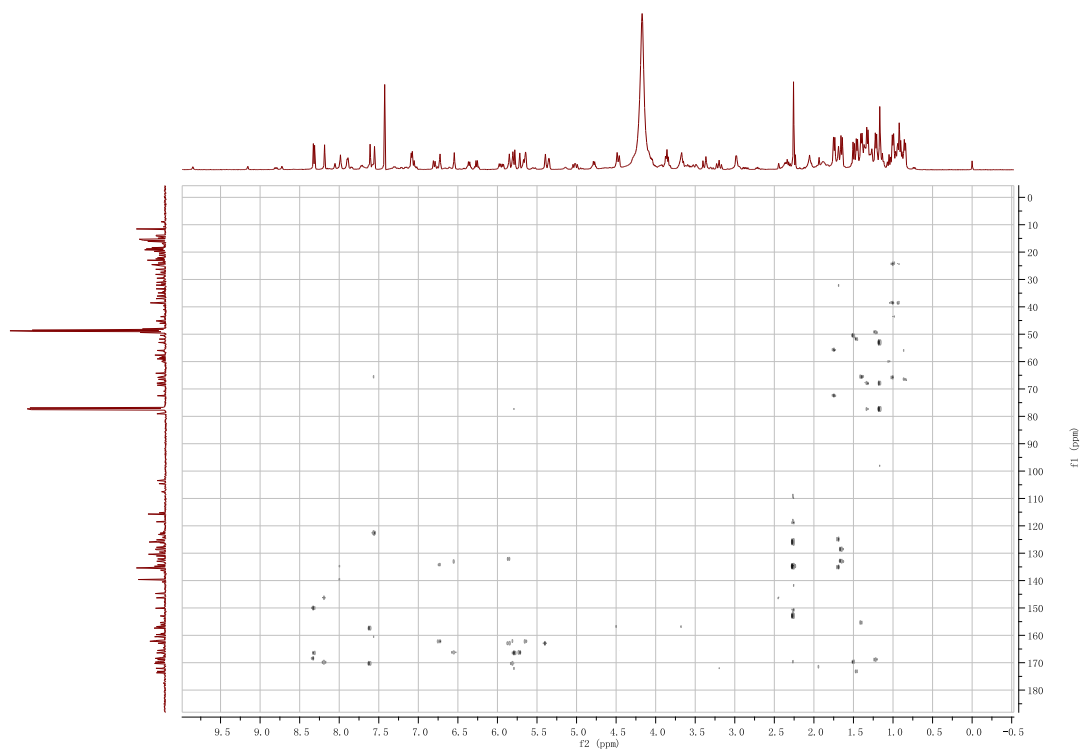
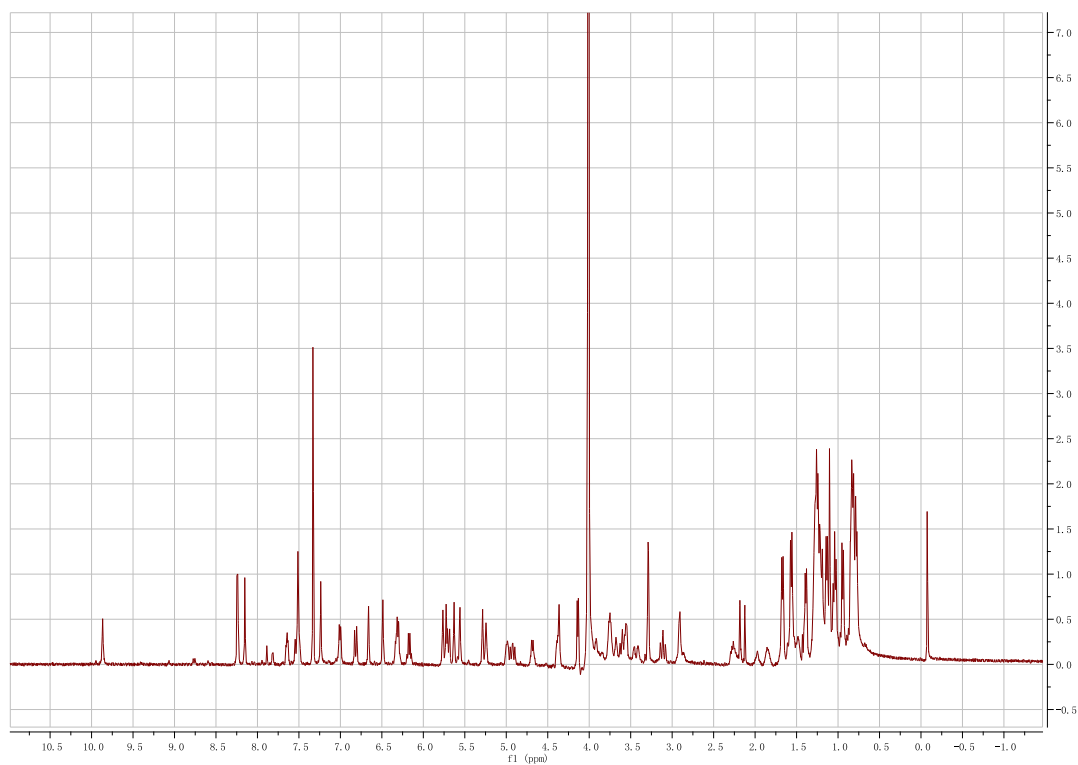
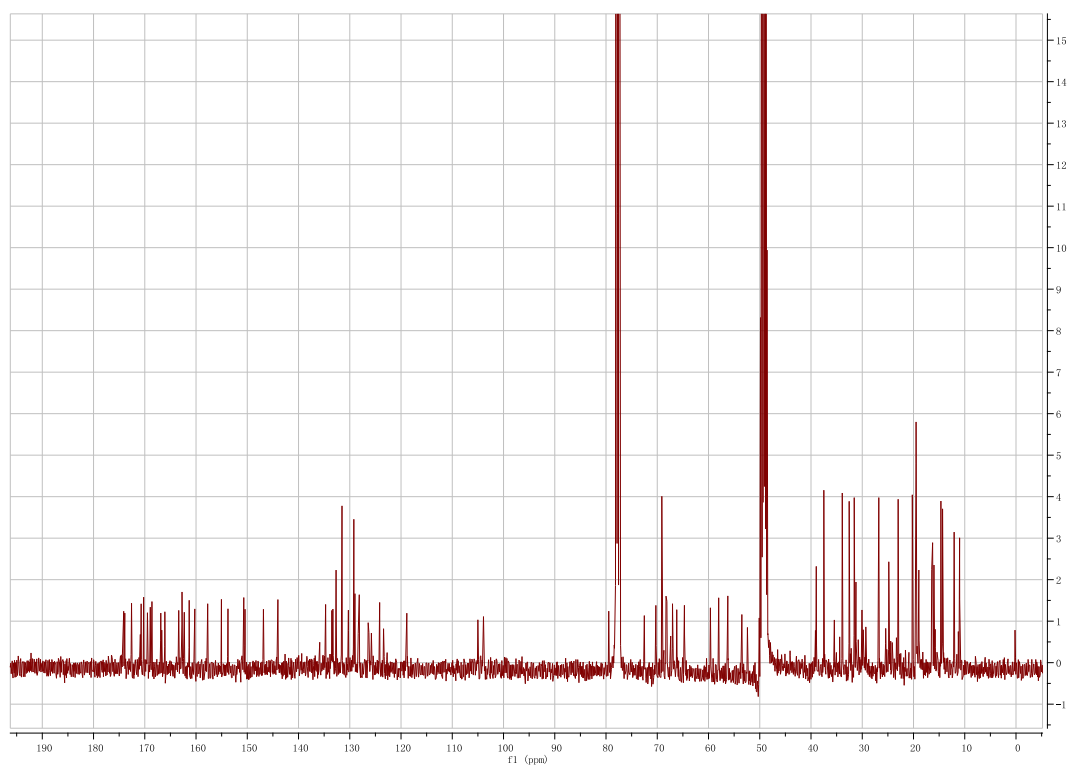


Fig. S6 1D and 2D NMR spectra of 12'-methyl-TSR

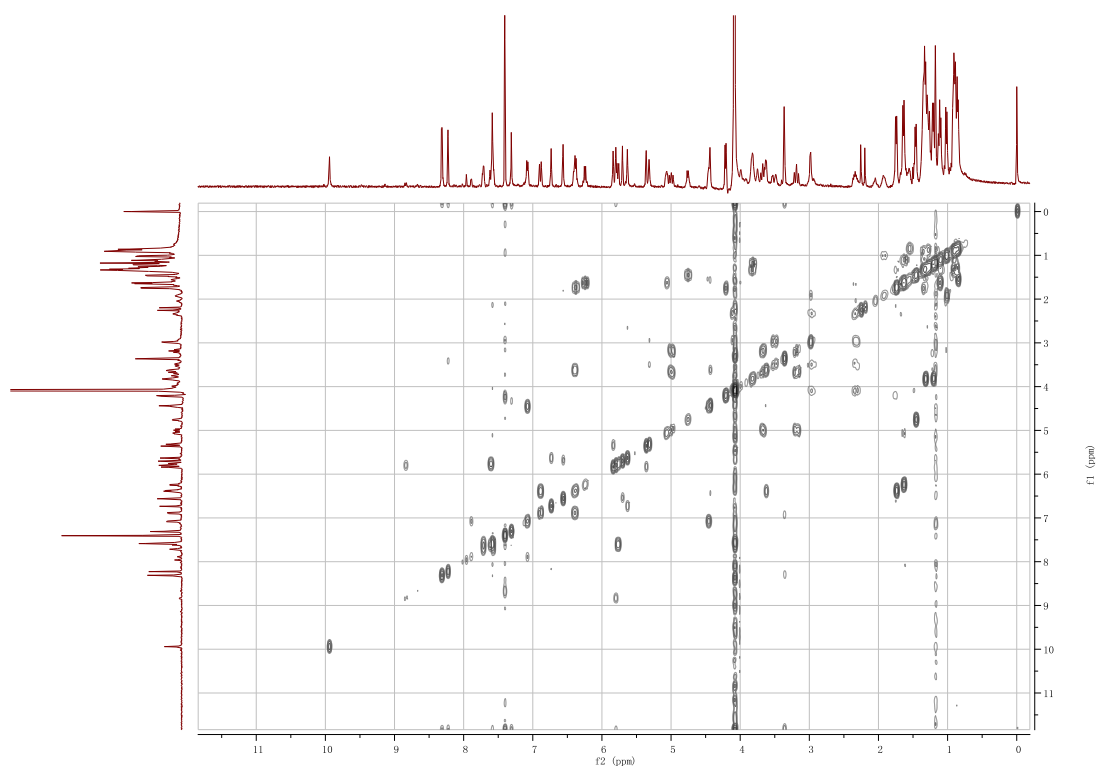
^1H NMR (400 MHz, $\text{CDCl}_3:\text{CD}_3\text{OD} = 4:1$)



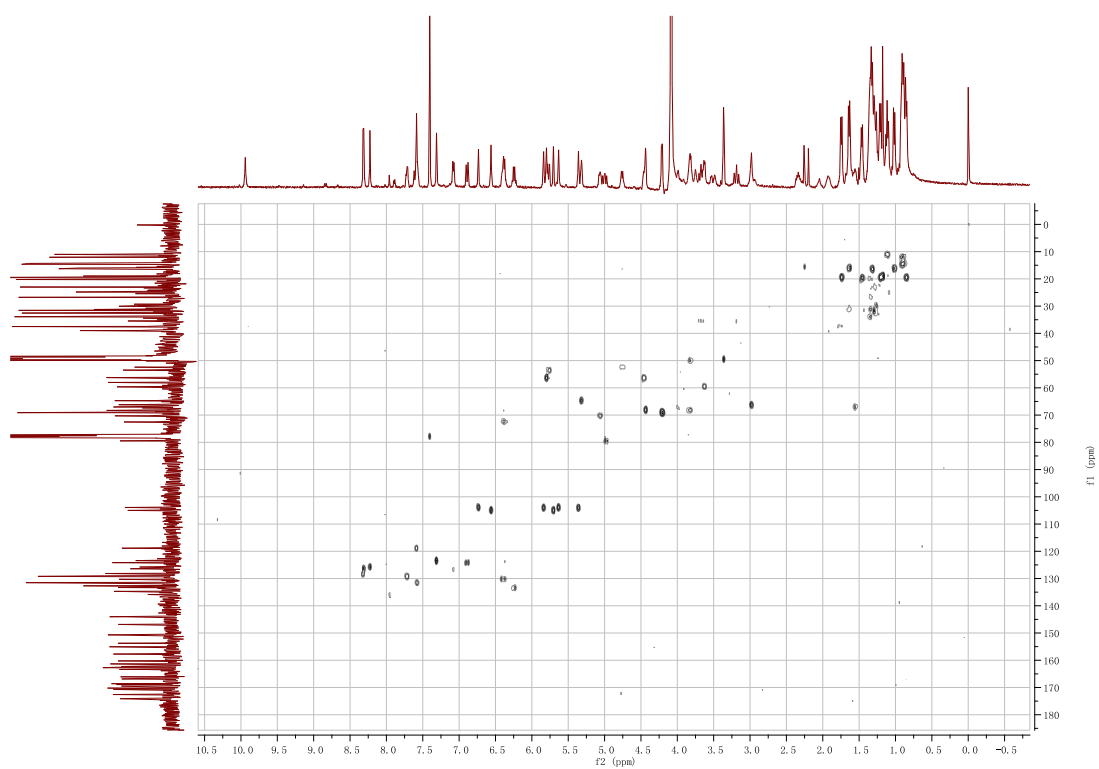
^{13}C NMR (100 MHz, $\text{CDCl}_3:\text{CD}_3\text{OD} = 4:1$)



gCOSY (400 MHz, CDCl₃:CD₃OD = 4:1)



gHMQC (400 MHz, CDCl₃:CD₃OD = 4:1)



gHMBC (400 MHz, CDCl₃:CD₃OD = 4:1)

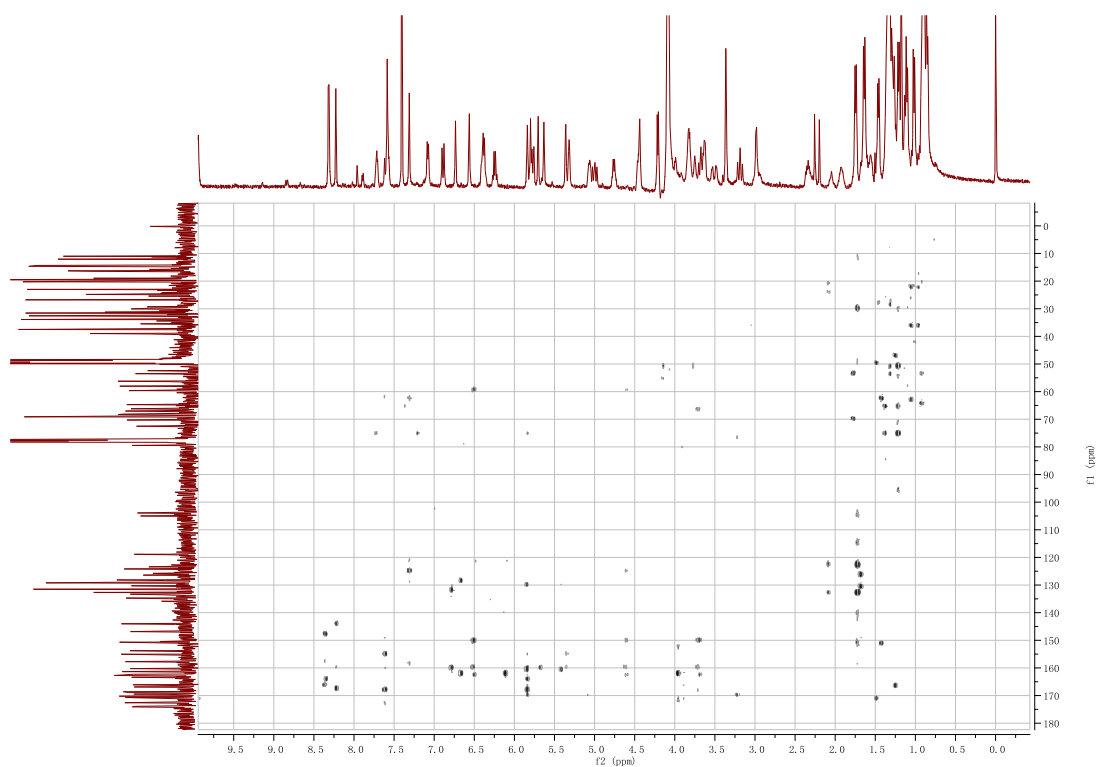
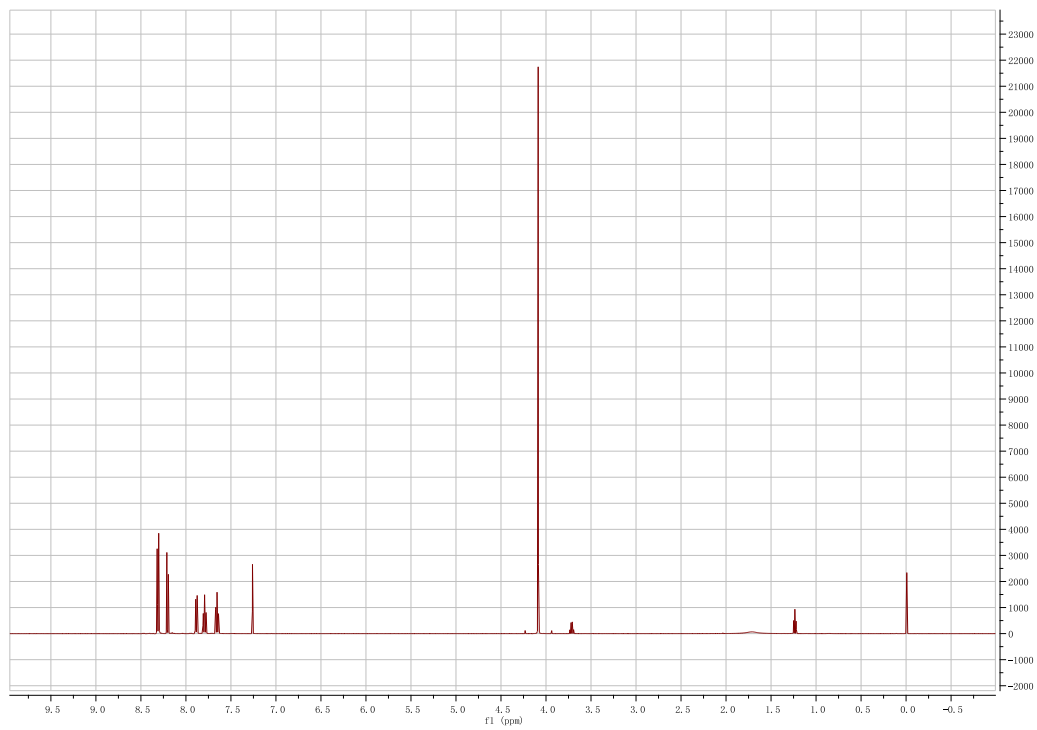


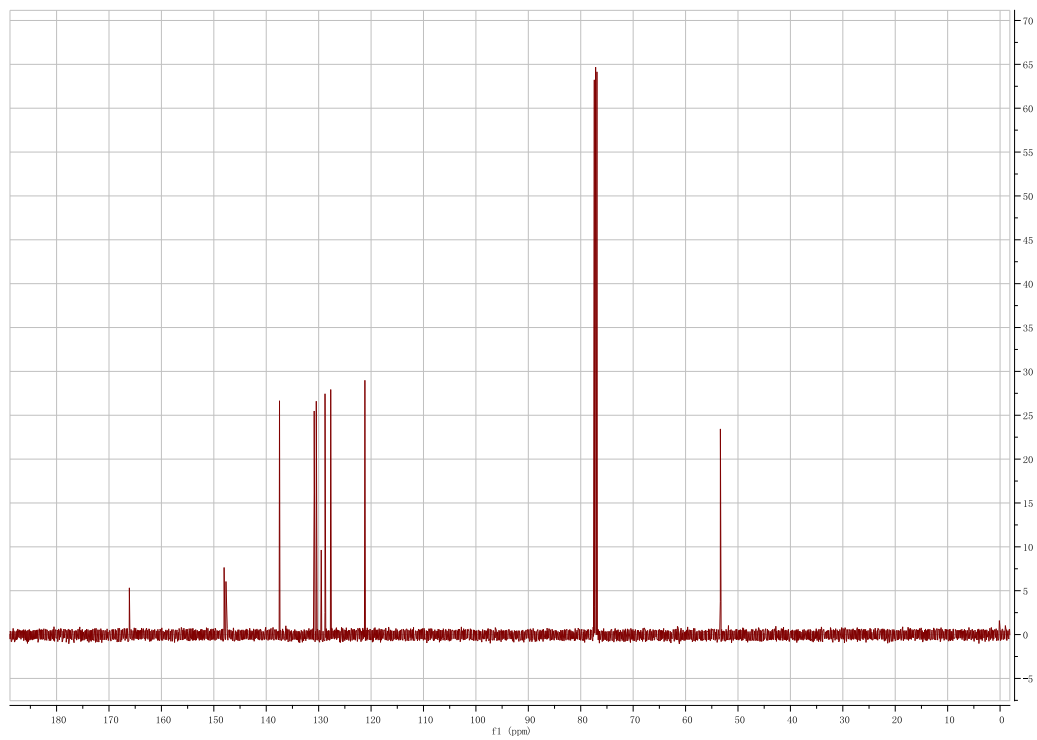
Fig. S7 NMR analysis of methyl quinoline-2-carboxylates and its analogues

(a) **1a**

^1H NMR (500 MHz, CDCl_3)

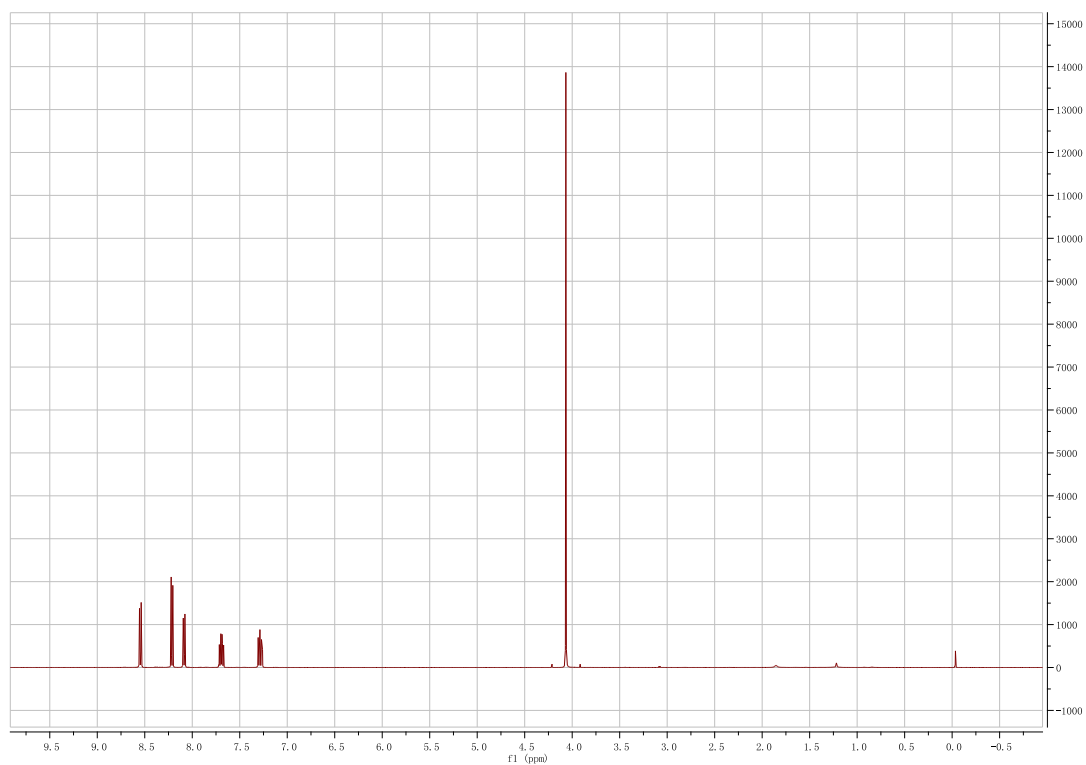


^{13}C NMR (125 MHz, CDCl_3)

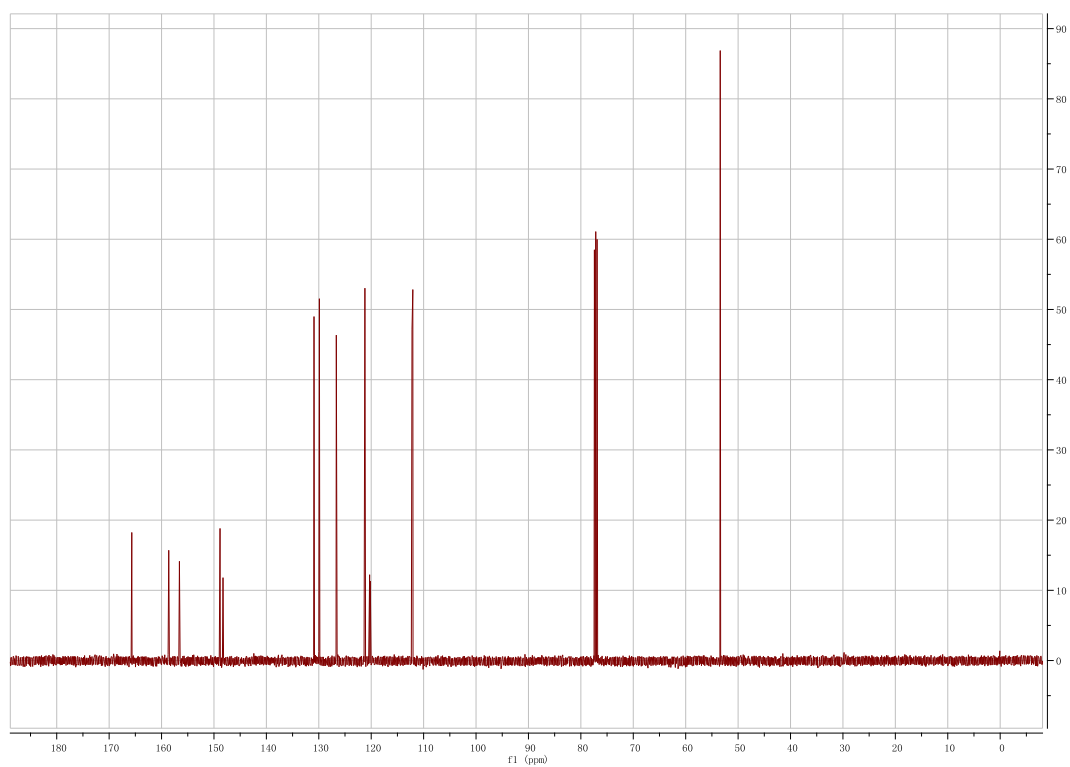


(b) **1b**

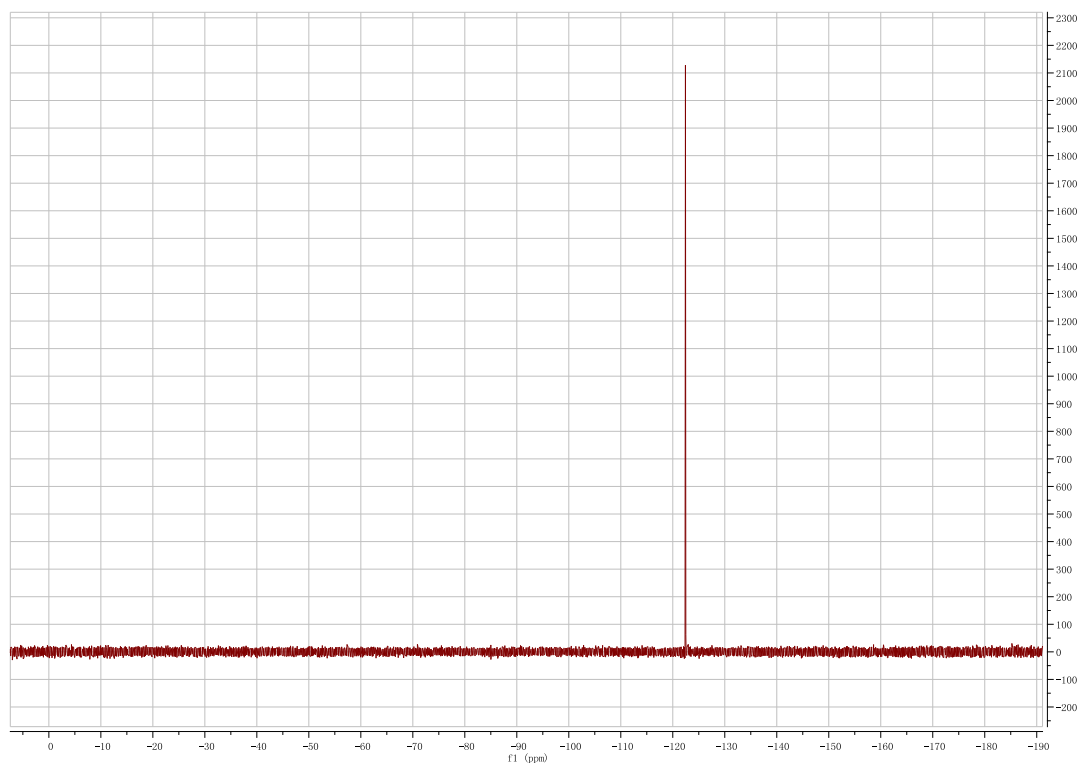
¹H NMR (500 MHz, CDCl₃)



¹³C NMR (125 MHz, CDCl₃)

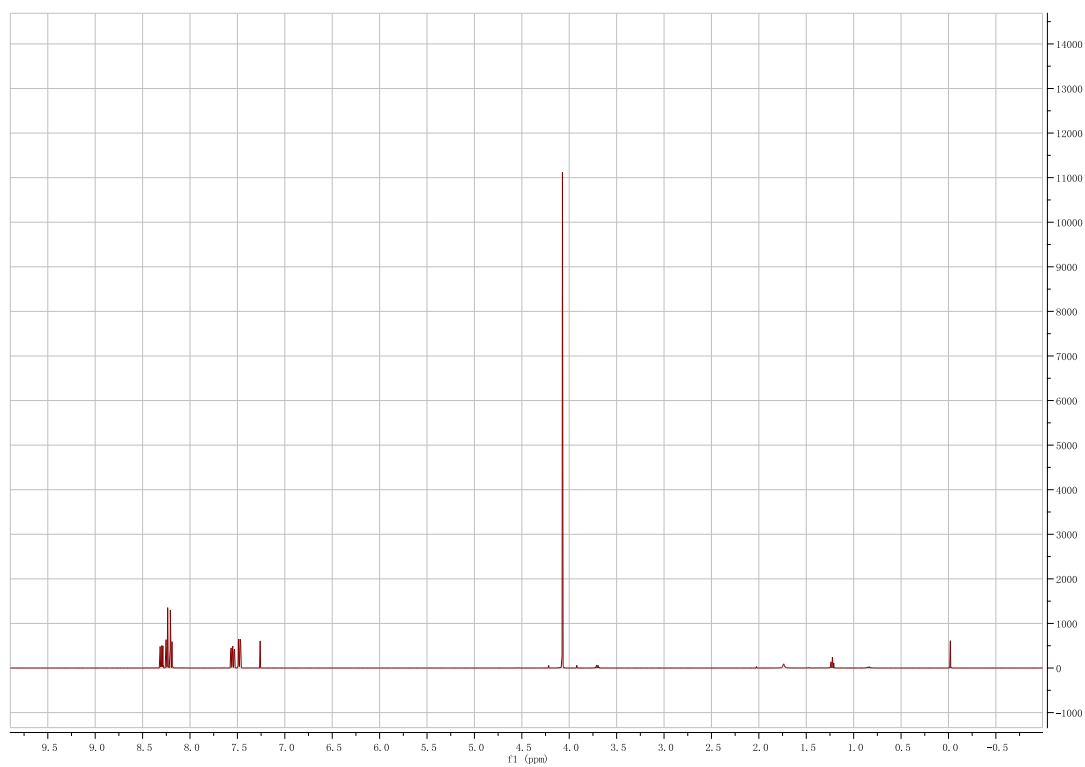


^{19}F NMR (282 MHz, CDCl_3)

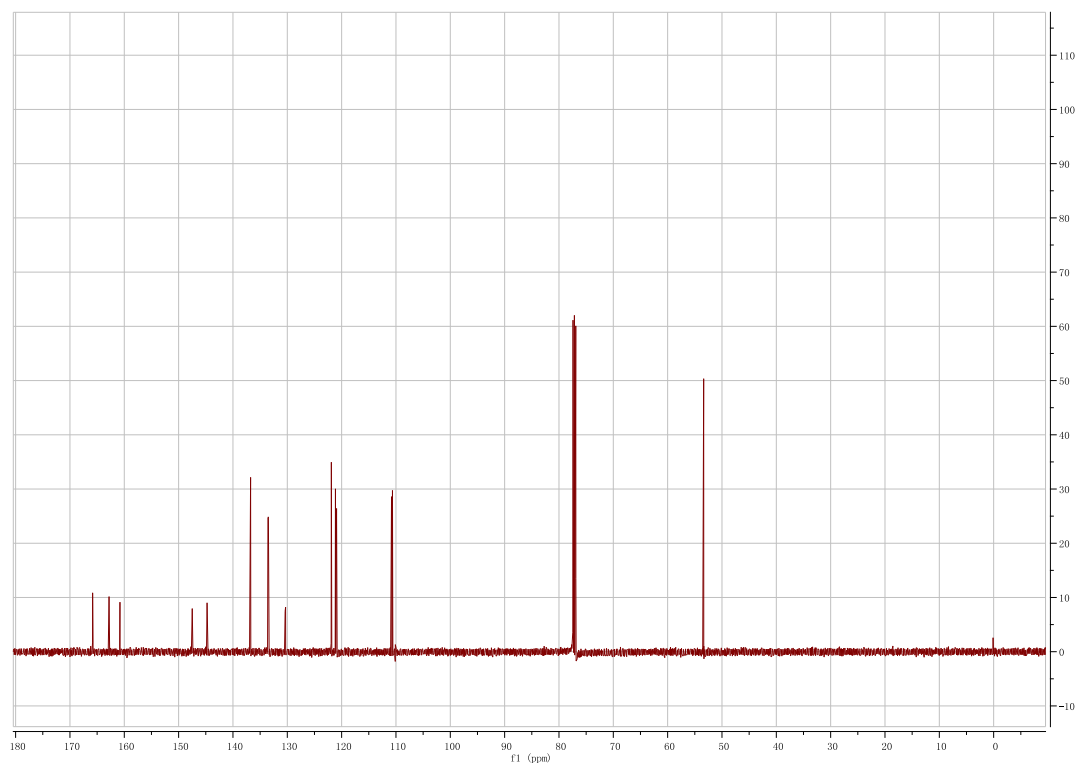


(c) **1c**

^1H NMR (500 MHz, CDCl_3)



^{13}C NMR (125 MHz, CDCl_3)



^{19}F NMR (282 MHz, CDCl_3)

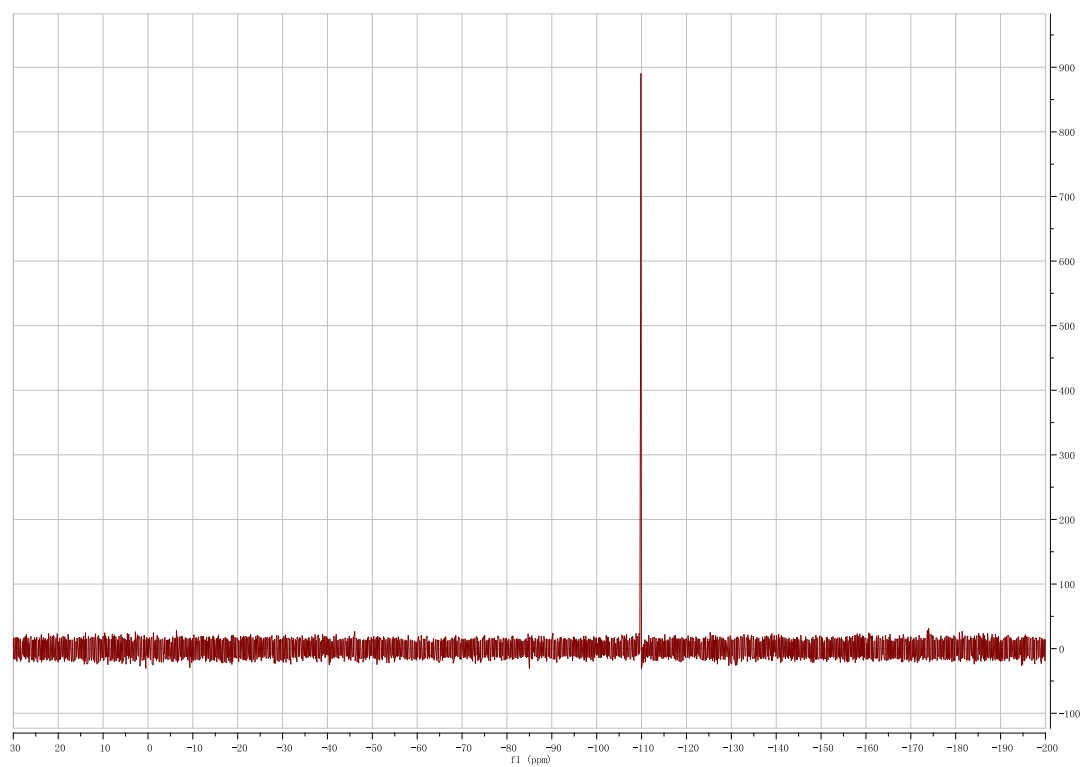
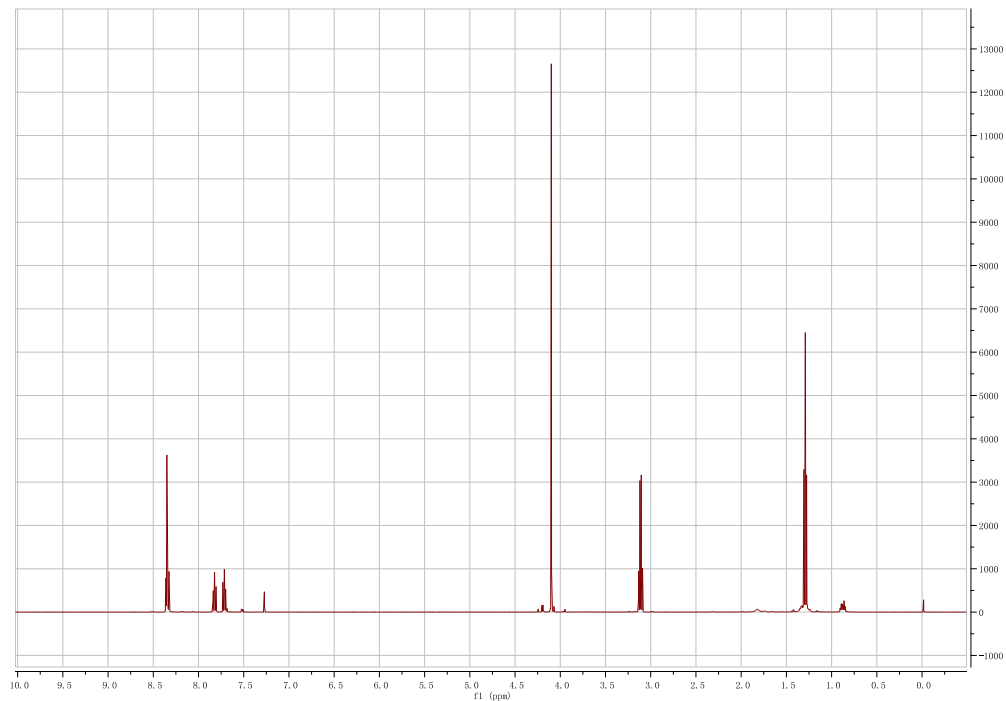


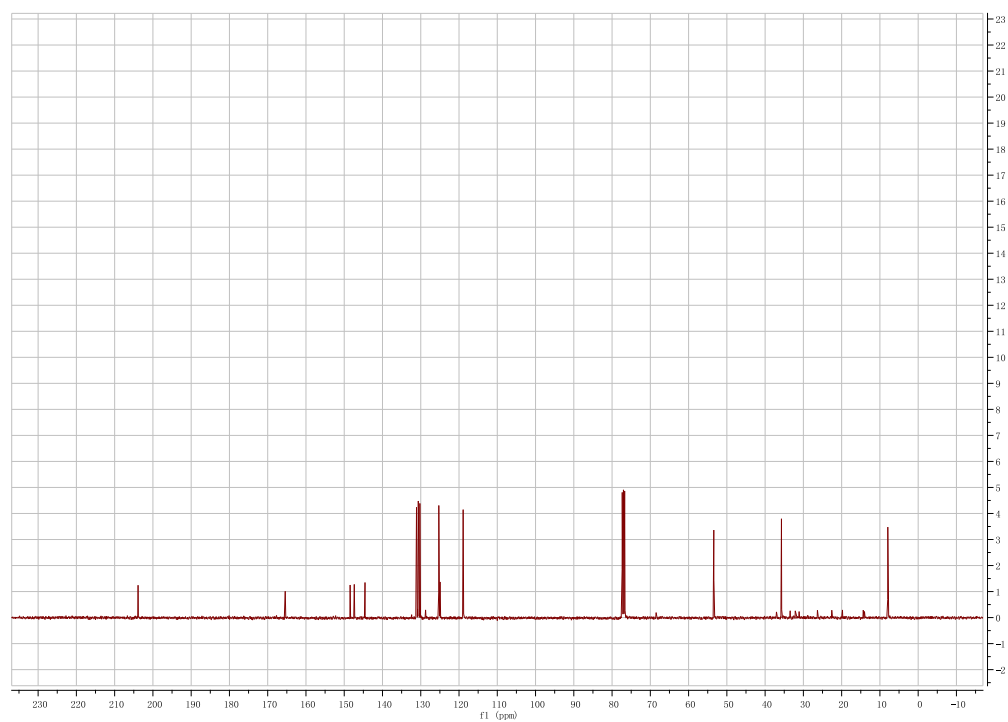
Fig. S8 NMR analysis of methyl 4-acetyl-quinoline-2-carboxylate and its analogues

(a) **2a**

^1H NMR (500 MHz, CDCl_3)

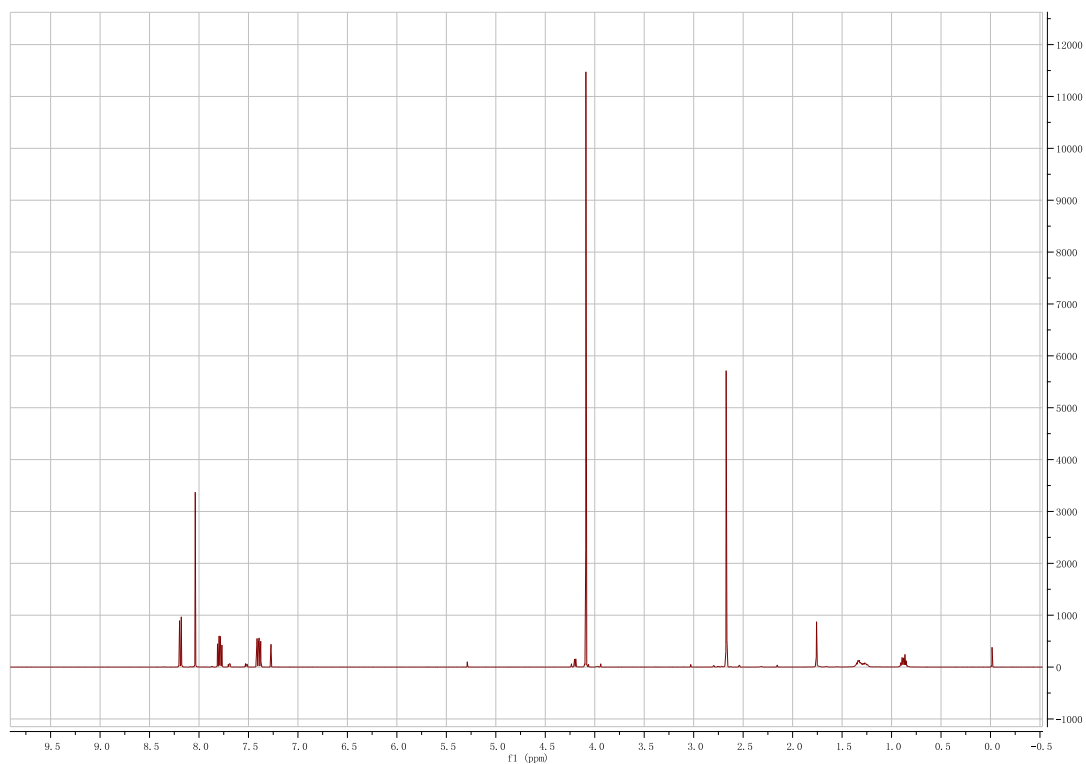


^{13}C NMR (125 MHz, CDCl_3)

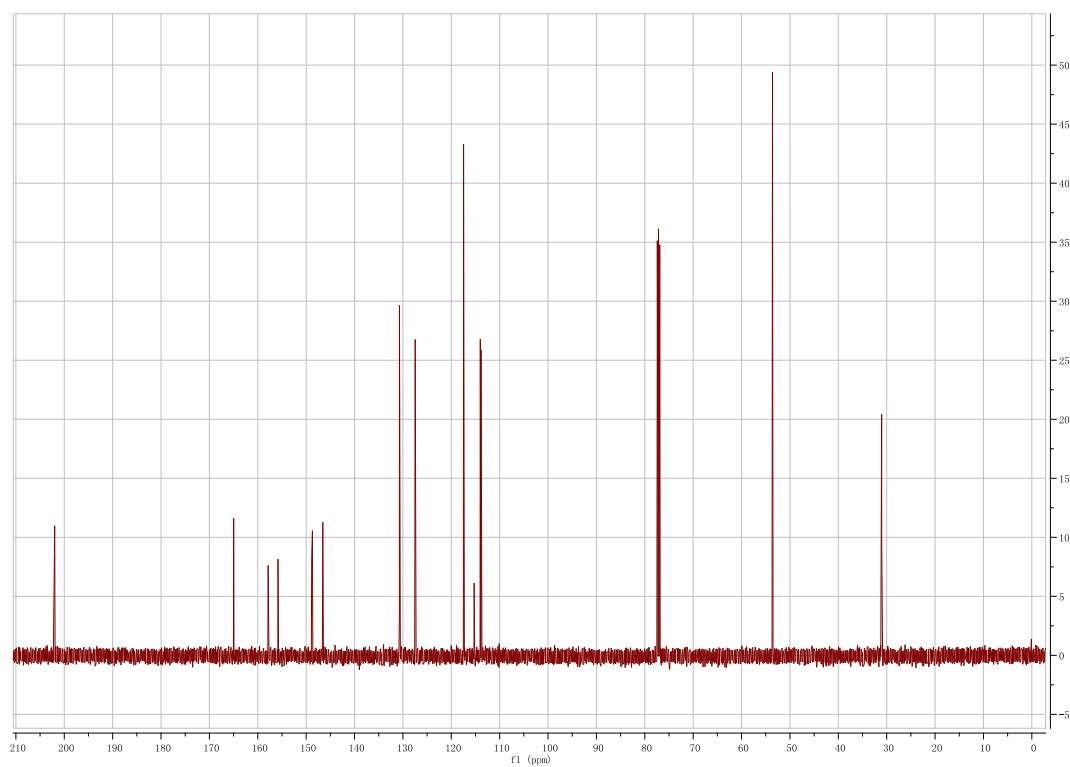


(b) **2b**

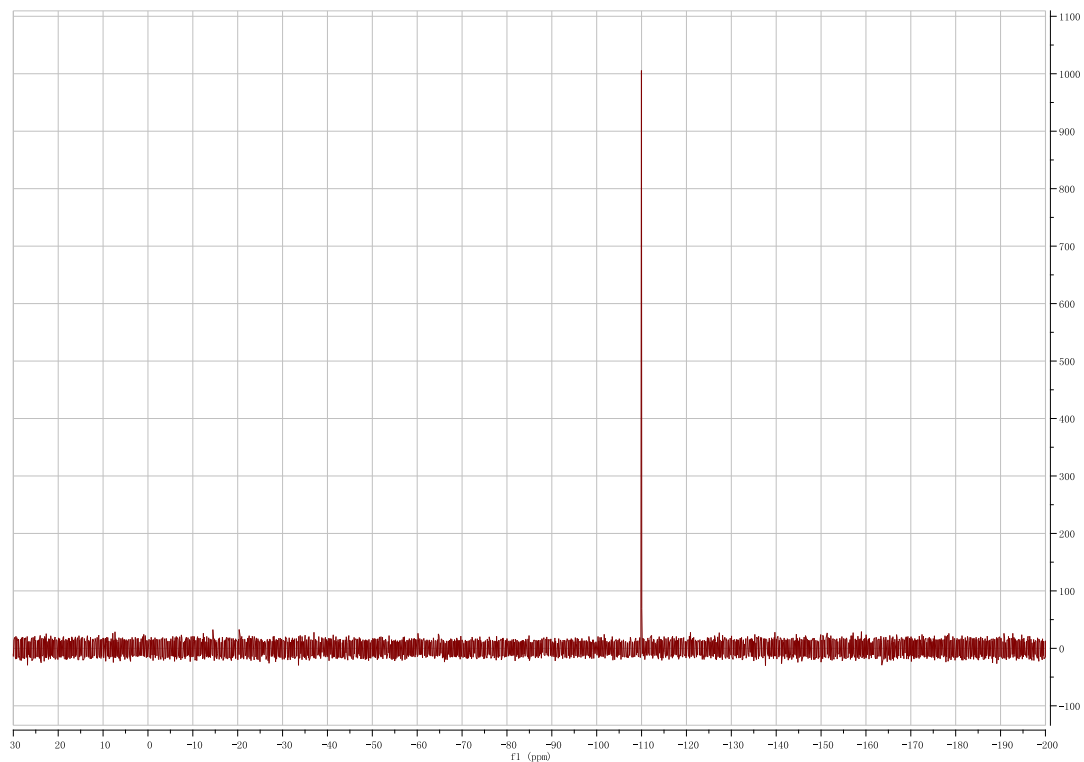
^1H NMR (500 MHz, CDCl_3)



^{13}C NMR (125 MHz, CDCl_3)

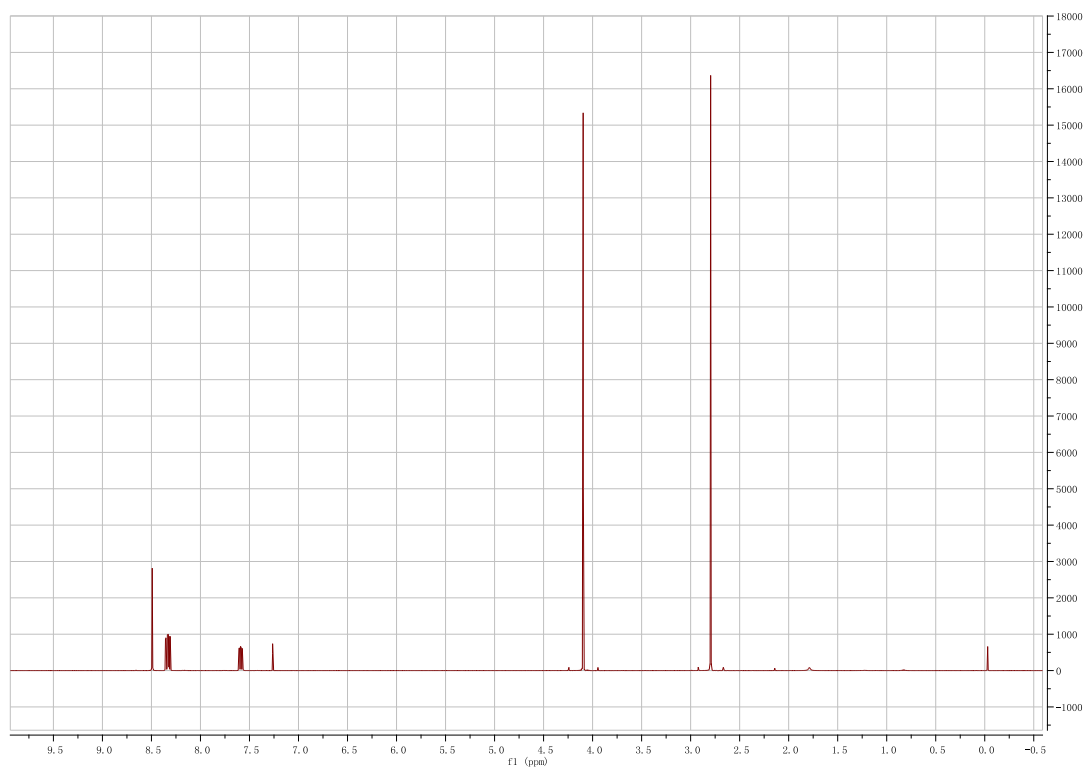


^{19}F NMR (282 MHz, CDCl_3)

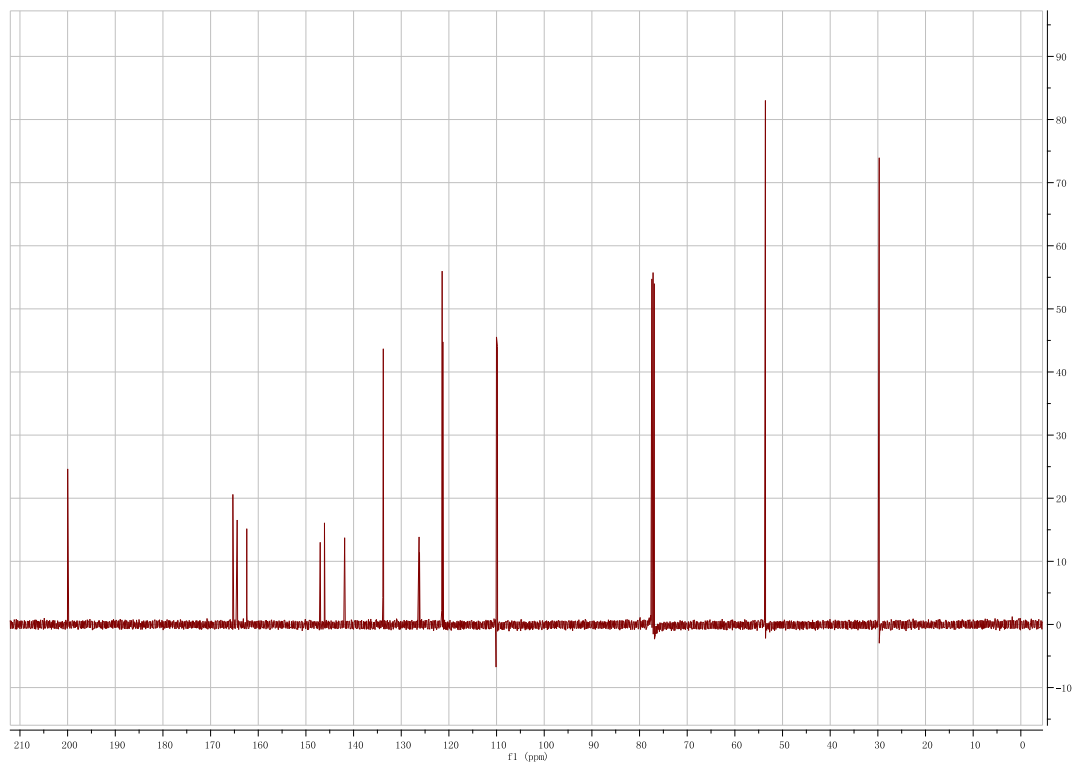


(c) **2c**

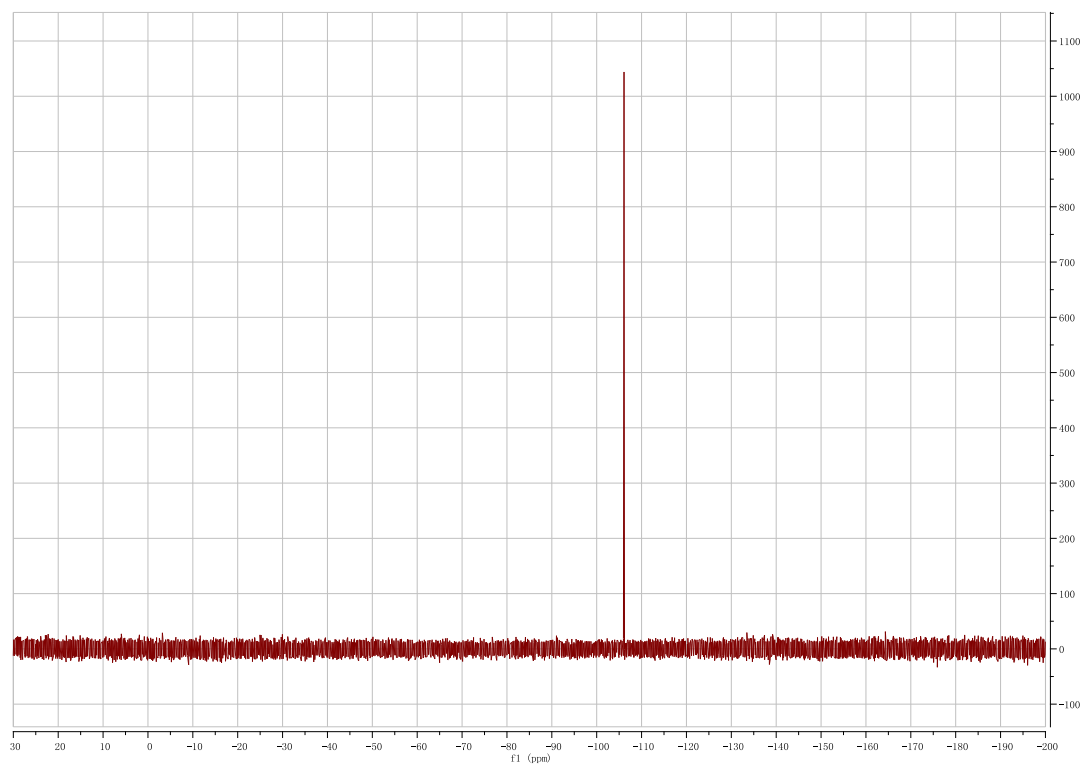
^1H NMR (500 MHz, CDCl_3)



^{13}C NMR (125 MHz, CDCl_3)



^{19}F NMR (282 MHz, CDCl_3)



3. Supplementary References

- 1 J. M. Harms, D. N. Wilson, F. Schluenen, S. R. Connell, T. Stachelhaus, Z. Zaborowska, C. M. T. Spahn and P. Fucini, *Mol. Cell*, 2008, **30**, 26.
- 2 M. Svensson, S. Humbel, R. D.J. Froese, T. Matsubara, S. Sieber and K. Morokuma, *J. Phys. Chem.*, 1996, **100**, 19357.
- 3 T. Vreven, K. Morokuma, O. Farkas, H. B. Schlege and M. J. Frisch, *J. Comput. Chem.*, 2003, **24**, 760.
- 4 Y. Zhao and D. G. Truhlar, *Theor. Chem. Acc.*, 2008, **120**, 215.
- 5 M. J. Frisch, et al. *Gaussian 09 (Revision A.02)*, Gaussian, Inc., Wallingford CT, 2009.
- 6 K. C. Nicolaou, M. Zak, B. S. Safina, A.A. Estrada, S.H. Lee and M. Nevalainen, *J. Am. Chem. Soc.*, 2005, **127**, 11176.
- 7 L. Duan, S. Wang, R. Liao and W. Liu, *Chem. Biol.*, 2012, **19**, 443.
- 8 R. Liao and W. Liu, *J. Am. Chem. Soc.*, 2011, **133**, 2852.
9. CLSI. Performance Standards for Antimicrobial Susceptibility Testing; Twenty-Second Informational Supplement. CLSI document M100-S21. Wayne, PA: Clinical and Laboratory Standards Institute. 2011.
10. U. Mocek, Z. Zeng, D. O'Hagan, P. Zhou, L.D.G. Fan, J. M. Beale and H. G. Floss, *J. Am. Chem. Soc.*, 1993, **115**, 7992.